

---

# MoMo: Momentum Models for Adaptive Learning Rates

---

Fabian Schaipp<sup>1</sup> Ruben Ohana<sup>2</sup> Michael Eickenberg<sup>2</sup> Aaron Defazio<sup>3</sup> Robert M. Gower<sup>2</sup>

## Abstract

Training a modern machine learning architecture on a new task requires extensive learning-rate tuning, which comes at a high computational cost. Here we develop new Polyak-type adaptive learning rates that can be used on top of any momentum method, and require less tuning to perform well. We first develop MoMo, a **Momentum Model** based adaptive learning rate for SGD-M (stochastic gradient descent with momentum). MoMo uses momentum estimates of the losses and gradients sampled at each iteration to build a model of the loss function. Our model makes use of any known lower bound of the loss function by using *truncation*, e.g. most losses are lower-bounded by zero. The model is then approximately minimized at each iteration to compute the next step. We show how MoMo can be used in combination with any momentum-based method, and showcase this by developing MoMo-Adam, which is Adam with our new model-based adaptive learning rate. We show that MoMo attains a  $\mathcal{O}(1/\sqrt{K})$  convergence rate for convex problems with interpolation, needing knowledge of no problem-specific quantities other than the optimal value. Additionally, for losses with unknown lower bounds, we develop on-the-fly estimates of a lower bound, that are incorporated in our model. We show that MoMo and MoMo-Adam improve over SGD-M and Adam in terms of robustness to hyperparameter tuning for training image classifiers on MNIST, CIFAR, and Imagenet, for recommender systems on Criteo, for a transformer model on the translation task IWSLT14, and for a diffusion model.

## 1. Introduction

Training a modern production-grade large neural network can cost over 1 million dollars in compute. For instance, the cost for the *Text-to-Text Transfer Transformer* T5-model (Raffel et al., 2020) is estimated to be more than 1.3 million dollars for a single run (Sharir et al., 2020). What makes training models highly expensive is that multiple runs are needed to tune the hyperparameters, with arguably the most important parameter being the learning rate. Indeed, finding a good learning-rate schedule plays a disproportionately large role in the resulting test error of the model, with one extensive study showing that it is of similar importance as the choice of optimizer (Schmidt et al., 2021).

Here, we develop adaptive learning rates that can be used together with any momentum-based method. To showcase our method, we apply our learning rates to SGD-M (stochastic gradient descent with momentum) and to Adam (Kingma & Ba, 2015), which gives the MoMo and MoMo-Adam method, respectively. We make use of model-based stochastic optimization (Asi & Duchi, 2019; Davis & Drusvyatskiy, 2019; Chadha et al., 2021), and leverage that loss functions are bounded below (typically by zero) to derive our new MoMo (**Momentum Model**) adaptive learning rate. An implementation of MoMo is available in `Pytorch` and `optax`.

### 1.1. The Model-Based Approach

Consider the problem

$$\min_{x \in \mathbb{R}^d} f(x), \quad f(x) := \mathbb{E}_{s \sim \mathcal{D}} [f(x, s)], \quad (1)$$

where  $f(x, s)$  is a loss function,  $s$  is an input (mini-batch of data), and  $x$  are the learnable parameters of a model. We assume throughout that  $f(x, s) \geq 0$ , which is true for most loss functions<sup>1</sup>. We also assume that  $f(\cdot, s)$  is continuously differentiable for all  $s \in \mathcal{D}$ , that there exists a solution  $x^*$  to (1) and denote the optimal value by  $f^* := f(x^*) \in \mathbb{R}$ .

In our main algorithms MoMo and MoMo-Adam (Algorithms 1 and 2), we present adaptive learning rates<sup>2</sup> for SGD-M and

<sup>1</sup>We choose zero as a lower bound for simplicity, but any constant lower bound could be handled.

<sup>2</sup>Here the term *adaptivity* refers to a scalar learning rate that changes from one iteration to the next by using easy-to-compute quantities.

---

<sup>1</sup>Department of Mathematics, Technical University of Munich, Munich <sup>2</sup>Flatiron Institute, CCM, New York <sup>3</sup>Meta AI, Fundamental AI Research (FAIR) team, New York. Correspondence to: Fabian Schaipp <fabian.schaipp@tum.de>.

Adam, respectively. To derive MoMo and MoMo-Adam, we use the model-based viewpoint, which is often motivated by the stochastic proximal point (SPP) (Asi & Duchi, 2019; Davis & Drusvyatskiy, 2019) method. At each iteration, SPP samples  $s_k \sim \mathcal{D}$ , then trades-off minimizing  $f(x, s_k)$  with not moving too far from the current iterate  $x^k$ . Given a learning rate  $\alpha_k > 0$ , this can be written as

$$x^{k+1} = \operatorname{argmin}_{x \in \mathbb{R}^d} f(x, s_k) + \frac{1}{2\alpha_k} \|x - x^k\|^2. \quad (2)$$

Since this problem needs to be solved at every iteration, it needs to be fast to compute. However, in general (2) is difficult to solve because  $f(x, s_k)$  can be a highly nonlinear function. Model-based methods replace  $f(x, s_k)$  by a simple model  $m_k(x)$  of the function (Asi & Duchi, 2019; Davis & Drusvyatskiy, 2019), and update according to

$$x^{k+1} = \operatorname{argmin}_{x \in \mathbb{R}^d} m_k(x) + \frac{1}{2\alpha_k} \|x - x^k\|^2. \quad (3)$$

SGD can be formulated as a model-based method by choosing the model to be the linearization of  $f(x, s_k)$  around  $x^k$ , that is

$$m_k(x) = f(x^k, s_k) + \langle \nabla f(x^k, s_k), x - x^k \rangle. \quad (4)$$

Using the above  $m_k(x)$  in (3) gives the SGD update

$$x^{k+1} = x^k - \alpha_k \nabla f(x^k, s_k),$$

see (Robbins & Monro, 1951; Asi & Duchi, 2019).

Our main insight for developing the MoMo methods is that we should build a model directly for  $f(x)$ , and not  $f(x, s_k)$ , since our objective is to minimize  $f(x)$ . To this end, we develop a model  $m_k(x)$  that is a good approximation of  $f(x)$  when  $x$  is close to  $x^k$ , and such that (3) has a closed-form solution. We use momentum estimates of past gradients and loss values to build a model  $f(x)$ . Finally, since the loss function is positive, we impose that our model be positive.

## 1.2. Background and Contributions

**Momentum and model-based methods.** The update formula of many stochastic methods such as SGD can be interpreted by taking a proximal step with respect to a model of the objective function (Asi & Duchi, 2019; Davis & Drusvyatskiy, 2019). Independently of this, (heavy-ball) momentum (Polyak, 1964; Sebbouh et al., 2021) is incorporated into many methods in order to boost performance.

*Contributions.* Here we give a new interpretation of momentum, namely that it can be motivated as a model of the objective function  $f(x)$  by averaging sampled loss functions. This allows us to naturally combine momentum with other model-based techniques.

**Lower bounds and truncated models.** One of the main advantages of the model-based viewpoint (Asi & Duchi, 2019; Davis & Drusvyatskiy, 2019) is that it illustrates how to use knowledge of a lower bound of the function via truncation. Methods using this truncated model are often easier to tune (Meng & Gower, 2023; Schaipp et al., 2023).

*Contributions.* By combining the model-based viewpoint of momentum with a truncated model we arrive at our new MoMo method. Since we are interested in loss functions, we can use zero as a lower bound estimate in many learning tasks. However, for some tasks such as training transformers, the minimal loss is often non-zero. If the non-zero lower bound is known, such as the entropy of language used in scaling laws (Kaplan et al., 2020), we can straightforwardly incorporate it into our model. For unknown lower bound values we also develop new online estimates of a lower bound in Section 4. Our estimates can be applied to any stochastic momentum-based method, and thus may be of independent interest. Our main influence for this technique was D-adaptation (Defazio & Mishchenko, 2023b) which develops an online estimate of the distance to the solution.

**Adaptive methods.** In practice, tuning the learning rate is intricate and computationally expensive. Adam (Kingma & Ba, 2015) (or AdamW (Loshchilov & Hutter, 2019)) is often easier to tune and now being used routinely to train DNNs across a variety of tasks. This and the success of Adam have incentivised the development of many new learning-rate techniques, including approaches based on coin-betting (Orabona & Tommasi, 2017), variants of AdaGrad (Duchi et al., 2011; Defazio & Mishchenko, 2023b), and stochastic line search (Vaswani et al., 2019). Recent work also combines parameter-free coin betting methods with truncated models (Chen et al., 2022).

*Contributions.* Our new adaptive learning rate can be combined with any momentum-based method, and allows for a preconditioner to be used. For example, Adam is a momentum method that makes use of a preconditioner. By using this viewpoint, together with a lower bound, we derive MoMo-Adam, a variant of Adam that uses our adaptive learning rates.

**Polyak step sizes.** For convex, non-smooth optimization, Polyak proposed an adaptive step size using the current objective function value  $f(x^k)$  and the optimal value  $f^*$  (Polyak, 1987). Recently, the Polyak step size has been adapted to the stochastic setting (Berrada et al., 2020; Gower et al., 2021; Loizou et al., 2021; Orvieto et al., 2022). For example, for  $c, \gamma_b > 0$  (Loizou et al., 2021) proposed

$$x^{k+1} = x^k - \min \left\{ \gamma_b, \frac{f(x^k, s_k) - \inf_z f(z, s_k)}{c \|\nabla f(x^k, s_k)\|^2} \right\} \nabla f(x^k, s_k),$$

called the SPS<sub>max</sub> method. The stochastic Polyak step size is closely related to stochastic model-based proximal point

methods as well as stochastic bundle methods (Asi & Duchi, 2019; Paren et al., 2022; Schaipp et al., 2023).

**Contributions.** Our proposed method MoMo can be seen as an extension of the Polyak step size that also incorporates momentum. This follows from the viewpoint of the Polyak step size (Berrada et al., 2020; Paren et al., 2022; Schaipp et al., 2023) as a truncated model-based method. In particular MoMo with no momentum is equal to  $\text{SPS}_{\max}$ .

**Numerical findings.** We find that MoMo consistently improves the sensitivity with respect to hyperparameter choice as compared to SGD-M. The same is true for MoMo-Adam compared to Adam. Our experiments cover image classification tasks on MNIST, CIFAR10, CIFAR100 and Imagenet, a recommender system for the Criteo dataset, an encoder-decoder transformer for the translation task IWSLT14, and a diffusion model.

Furthermore, we find that the adaptive learning rate of MoMo(-Adam) for some tasks automatically performs a warm-up at the beginning of training and a decay in later iterations, two techniques often used to improve training (Sun, 2020).

## 2. Model-Based Momentum Methods

Let us recall the SGD model in (4) which has two issues: first, it approximates a single stochastic function  $f(x, s_k)$ , as opposed to the full loss  $f(x)$ . Second, this model can be negative even though our loss function is always positive. Here, we develop a model directly for  $f(x)$ , and not  $f(x, s_k)$ , which also takes into account lower bounds on the function value.

### 2.1. Model-Based Viewpoint of Momentum

Suppose we have sampled inputs  $s_1, \dots, s_k$  and past iterates  $x^1, \dots, x^k$ . We can use these samples to build a model of  $f(x)$  by averaging past function evaluations as follows

$$f(x) = \mathbb{E}_{s \sim \mathcal{D}} [f(x, s)] \approx \frac{1}{\rho_k} \sum_{j=1}^k \rho_{j,k} f(x, s_j), \quad (5)$$

where  $\rho_{j,k} \geq 0$  and  $\rho_k := \sum_{j=1}^k \rho_{j,k}$ . Thus, the  $\rho_k^{-1} \rho_{j,k}$  are a discrete probability mass function over the previous samples. The issue with (5) is that it is expensive to evaluate  $f(x, s_j)$  for  $j = 1, \dots, k$ , which we would need to do at every iteration. Instead, we approximate each  $f(x, s_j)$  by linearizing  $f(x, s_j)$  around  $x^j$ , the point it was last evaluated, that is for  $j = 1, \dots, k$

$$f(x, s_j) \approx f(x^j, s_j) + \langle \nabla f(x^j, s_j), x - x^j \rangle. \quad (6)$$

Using (5) and the linear approximations in (6) we can approximate  $f(x)$  with the model  $m_k(x)$  given by

$$m_k^{\text{avg}}(x) = \frac{1}{\rho_k} \sum_{j=1}^k \rho_{j,k} (f(x^j, s_j) + \langle \nabla f(x^j, s_j), x - x^j \rangle). \quad (7)$$

If we plug in the above model  $m_k^{\text{avg}}(x)$  into (3), then the resulting update is given by

$$x^{k+1} = x^k - \frac{\alpha_k}{\rho_k} d_k, \quad d_k := \sum_{j=1}^k \rho_{j,k} \nabla f(x^j, s_j). \quad (8)$$

By appropriately choosing the  $\rho_{j,k}$  (details in Section 2.3), the above method is equivalent to SGD-M. This gives a new viewpoint of (heavy-ball) momentum. Next we incorporate a lower bound into this model so that, much like the loss function, it cannot become negative.

### 2.2. Deriving MoMo

Since we know the loss is lower-bounded by zero, we will also impose a lower bound on the model (7). Though we could use zero, we will use an estimate  $f_*^k \geq 0$  of the lower bound to allow for cases where  $f(x^*)$  may be far from zero. Imposing a lower bound of  $f_*^k$  gives the following model

$$f(x) \approx \max \left\{ m_k^{\text{avg}}(x), f_*^k \right\} =: m_k(x). \quad (9)$$

For overparametrized machine-learning models the minimum value  $f(x^*)$  is often close to zero (Ma et al., 2018; Gower et al., 2021). Thus, choosing  $f_*^k = 0$  in every iteration will work well (as we verify later in our experiments). For tasks where  $f_*^k = 0$  is too loose of a bound, in Section 4 we develop an online estimate for  $f_*^k$  based on available information. Using the model (9), we can now define the proximal update

$$x^{k+1} = \operatorname{argmin}_{y \in \mathbb{R}^d} m_k(y) + \frac{1}{2\alpha_k} \|y - x^k\|^2. \quad (10)$$

Because  $m_k(y)$  is a simple piece-wise linear function, the update (10) has a closed form solution, as we show in the following lemma (proof in Appendix C.1).

**Lemma 2.1.** [MoMo update] Let

$$\begin{aligned} d_k &:= \sum_{j=1}^k \rho_{j,k} \nabla f(x^j, s_j), \\ \bar{f}_k &:= \sum_{j=1}^k \rho_{j,k} f(x^j, s_j), \\ \gamma_k &:= \sum_{j=1}^k \rho_{j,k} \langle \nabla f(x^j, s_j), x^j \rangle. \end{aligned} \quad (11)$$

Using model (9), the closed form solution to (10) is

$$\begin{aligned} \tau_k &:= \min \left\{ \frac{\alpha_k}{\rho_k}, \frac{(\bar{f}_k + \langle d_k, x^k \rangle - \gamma_k - \rho_k f_*^k)_+}{\|d_k\|^2} \right\}, \\ x^{k+1} &= x^k - \tau_k d_k. \end{aligned} \quad (12)$$

Finally, it remains to select the averaging coefficients  $\rho_{j,k}$ . Here we will use an exponentially weighted average that places more weight on recent samples. Aside from working well in practice on countless real-world examples, exponential averaging can be motivated through the model-based interpretation. Recent iterates will most likely have gradients and loss values that are closer to the current iterate  $x^k$ . Thus, we place more weight on recent iterates, i.e.  $\rho_{j,k}$  is big for  $j$  close to  $k$ . We give two options for exponentially weighted averaging next.

### 2.3. The Coefficients $\rho_{j,k}$ : To bias or not to bias

We now choose  $\rho_{j,k} \geq 0$  such that we can update  $\bar{f}_k$ ,  $d_k$  and  $\gamma_k$  in (11) on the fly, storing only two scalars and one vector, resulting in the same iteration complexity as SGD-M.

**Exponentially Weighted Average.** Let  $\beta \in [0, 1)$ . Starting with  $\rho_{1,1} = 1$ , and for  $k \geq 2$  define

$$\rho_{j,k} = \begin{cases} \beta \rho_{j,k-1}, & j \leq k-1, \\ 1 - \beta, & j = k. \end{cases}$$

Then,  $\rho_k = \sum_{j=1}^k \rho_{j,k} = 1$  for all  $k \in \mathbb{N}$  and the quantities in (11) are exponentially weighted averages, see Lemma A.1. As a consequence, we can update  $\bar{f}_k$ ,  $d_k$  and  $\gamma_k$  on the fly as given in lines 5–7 in Algorithm 1. Combining update (12) and  $\rho_k = 1$ , we obtain Algorithm 1, which we call MoMo.

---

**Algorithm 1** MoMo: Model-based Momentum method.

---

- 1: **Default settings:**  $\alpha_k = 1, \beta = 0.9, (f_*^k)_{k \in \mathbb{N}} = 0$ .
  - 2: **Input:**  $x^1 \in \mathbb{R}^d, \beta \in [0, 1), \alpha_k > 0, (f_*^k)_{k \in \mathbb{N}} \subset \mathbb{R}$
  - 3: **Init:**  $\bar{f}_0 = f(x^1, s_1), d_0 = \nabla f(x^1, s_1), \gamma_0 = \langle d_0, x^1 \rangle$
  - 4: **for**  $k = 1$  **to**  $K - 1$  **do**
  - 5:    $\bar{f}_k = (1 - \beta)f(x^k, s_k) + \beta\bar{f}_{k-1}$
  - 6:    $\gamma_k = (1 - \beta)\langle \nabla f(x^k, s_k), x^k \rangle + \beta\gamma_{k-1}$
  - 7:    $d_k = (1 - \beta)\nabla f(x^k, s_k) + \beta d_{k-1}$
  - 8:    $h_k = \bar{f}_k + \langle d_k, x^k \rangle - \gamma_k$
  - 9:    $x^{k+1} = x^k - \min \left\{ \alpha_k, \frac{(h_k - f_*^k)_+}{\|d_k\|^2} \right\} d_k$
  - 10: **end for**
- 

**Remark 2.2.** The *adaptive learning rate*  $\tau_k$  in (12) determines the size of the step and can vary in each iteration even if  $\alpha_k$  is constant. The (*user-specified*) *learning rate*  $\alpha_k$  caps the adaptive learning rate.

**Remark 2.3 (Complexity).** MoMo has the same order iteration complexity and memory footprint as SGD-M. MoMo stores two additional scalars  $\gamma_k$  and  $\bar{f}_k$ , as compared to SGD-M, and has two additional  $\mathcal{O}(d)$  inner products lines 6 and 8, and one  $\mathcal{O}(d)$  vector norm on line 9.

For  $\beta = 0$  (no momentum), we have  $\gamma_k = \langle \nabla f(x^k, s_k), x^k \rangle = \langle d_k, x^k \rangle$  and  $\bar{f}_k = f(x^k, s_k)$ . Consequently  $h_k = f(x^k, s_k)$ , and in this special case, MoMo is equivalent<sup>3</sup> to SPS<sub>max</sub>.

Figure 1 shows how the MoMo model (9) approximates a convex function (left) and a non-convex function (right). The MoMo update  $x_{\text{MoMo}}^{k+1}$  in Figure 1 attains a smaller loss for both examples, as compared to the SGD-M update.

**Averaging with Bias Correction.** Alternatively, we can choose  $\rho_{j,k} = (1 - \beta)\beta^{k-j}$  for  $j = 1, \dots, k$ , as it is used in Adam (Kingma & Ba, 2015). This gives  $\rho_k = 1 - \beta^k \neq 1$ . We discuss this choice for MoMo in Appendix A.1 and for consistencies sake will use it later for MoMo-Adam.

## 3. Weight Decay and Preconditioning

Often weight decay is used in order to improve generalization (Zhang et al., 2019). Weight decay is equivalent to adding a squared  $\ell_2$ -regularization to the objective function (Krogh & Hertz, 1991), in other words, instead of (1) we solve  $\min_{x \in \mathbb{R}^d} f(x) + \frac{\lambda}{2} \|x\|^2$ , where  $f(x)$  is again the loss function. To include weight decay, we build a model  $m_k$  for the loss  $f$  and keep the  $\ell_2$ -regularization outside of the model. That is equation (10) is modified to

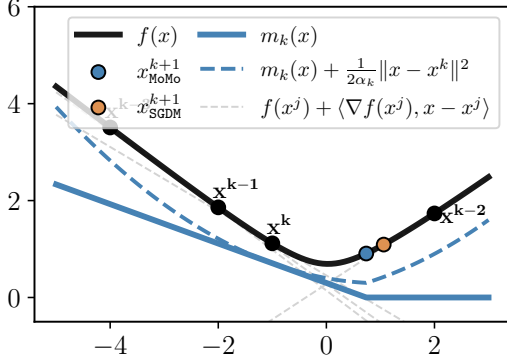
$$x^{k+1} = \operatorname{argmin}_{y \in \mathbb{R}^d} m_k(y) + \frac{\lambda}{2} \|y\|^2 + \frac{1}{2\alpha_k} \|y - x^k\|^2. \quad (13)$$

Finally, the Euclidean norm may often not be best suited. Many popular methods such as AdaGrad or Adam can be interpreted as using a preconditioner for the proximal step. Hence, we allow for an arbitrary norm defined by a symmetric, positive definite matrix  $\mathbf{D}_k \in \mathbb{R}^{d \times d}$ , i.e.  $\|x\|_{\mathbf{D}_k}^2 := \langle \mathbf{D}_k x, x \rangle$ . We can now use  $\mathbf{D}_k$  to change the metric within our proximal method, by updating

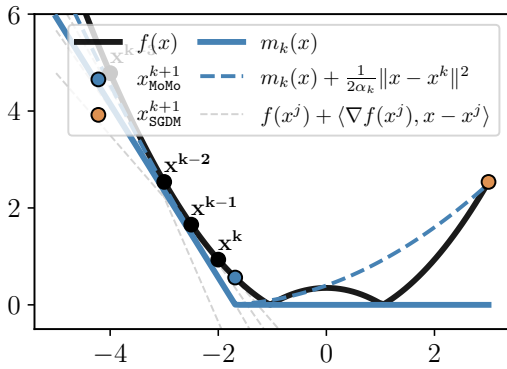
$$x^{k+1} = \operatorname{argmin}_{y \in \mathbb{R}^d} m_k(y) + \frac{\lambda}{2} \|y\|_{\mathbf{D}_k}^2 + \frac{1}{2\alpha_k} \|y - x^k\|_{\mathbf{D}_k}^2. \quad (14)$$

This update (14) enjoys the following closed form solution (proof in Appendix C.2).

<sup>3</sup>This equivalence requires setting  $\gamma_b \leftarrow \alpha_k, c \leftarrow 1$ , and assuming  $f_*^k = \inf_z f(z, s_k)$ .



(a) Convex loss



(b) Non-convex loss

Figure 1. Illustration of the MoMo model (blue curves) for two different loss functions with  $\alpha_k = 5$ . Due to truncation, the new iterate of MoMo (blue point) is closer to the minimum than SGD-M (orange point). The right plot shows how MoMo takes a small step when gradients are steep, whereas SGD-M takes a large step and ends up far from the solution.

**Lemma 3.1.** Using model (9), the closed form solution to (14) is given by

$$\tau_k = \min \left\{ \frac{\alpha_k}{\rho_k}, \frac{((1+\alpha_k\lambda)(\bar{f}_k - \rho_k f_*^k - \gamma_k) + \langle d_k, x^k \rangle)_+}{\|d_k\|_{\mathbf{D}_k^{-1}}^2} \right\}, \quad (15)$$

$$x^{k+1} = \frac{1}{1+\alpha_k\lambda} \left[ x^k - \tau_k \mathbf{D}_k^{-1} d_k \right]. \quad (16)$$

Lemma 3.1 shows how to incorporate weight decay in MoMo: we replace line 9 in Algorithm 1 by (15)-(16) with  $\mathbf{D}_k = \mathbf{I}_d$  and  $\rho_k = 1$ . If  $\beta = 0$  (no momentum) then MoMo with weight decay recovers ProxSPS, the proximal version of the stochastic Polyak step size (Schaipp et al., 2023).

**Deriving MoMo-Adam.** Using Lemma 3.1 we can obtain an Adam-version of MoMo by defining  $\mathbf{D}_k$  as the diagonal preconditioner of Adam. Let  $\mathbf{1}_d$  be the  $d$ -dimensional vector

**Algorithm 2** MoMo-Adam: Adaptive learning rates for Adam

- 1: **Default settings:**  $\alpha_k = 10^{-2}$ ,  $(\beta_1, \beta_2) = (0.9, 0.999)$ ,  $\epsilon = 10^{-8}$
- 2: **Input:**  $x^1 \in \mathbb{R}^d$ ,  $\beta_1, \beta_2 \in [0, 1)$ ,  $\epsilon > 0$ ,  $\alpha_k > 0$ ,  $\lambda \geq 0$ , and  $(f_*^k)_{k \in \mathbb{N}} \subset \mathbb{R}$ .
- 3: **Initialize:**  $\bar{f}_0 = 0, d_0 = 0, \gamma_0 = 0$ , and  $v_0 = 0$ .
- 4: **for**  $k = 1$  **to**  $K - 1$  **do**
- 5:  $g_k = \nabla f(x^k, s_k)$ ;  $d_k = (1 - \beta_1)g_k + \beta_1 d_{k-1}$
- 6:  $v_k = \beta_2 v_{k-1} + (1 - \beta_2)(g_k \odot g_k)$
- 7:  $\mathbf{D}_k = \text{Diag}(\epsilon \mathbf{1}_d + \sqrt{v_k / (1 - \beta_2^k)})$
- 8:  $\bar{f}_k = (1 - \beta_1)f(x^k, s_k) + \beta_1 \bar{f}_{k-1}$
- 9:  $\gamma_k = (1 - \beta_1)\langle g_k, x^k \rangle + \beta_1 \gamma_{k-1}$
- 10:  $h_k = \frac{((1+\lambda\alpha_k)(\bar{f}_k - \gamma_k - (1-\beta_1^k)f_*^k) + \langle d_k, x^k \rangle)_+}{\|d_k\|_{\mathbf{D}_k^{-1}}^2}$
- 11:  $\tau_k = \min \left\{ (1 - \beta_1^k)^{-1} \alpha_k, h_k \right\}$
- 12:  $x^{k+1} = \frac{1}{1+\alpha_k\lambda} \left[ x^k - \tau_k \mathbf{D}_k^{-1} d_k \right]$
- 13: **end for**

of ones,  $\text{Diag}(v)$  a diagonal matrix with diagonal entries  $v \in \mathbb{R}^d$ , and  $\odot$  and  $\sqrt{\cdot}$  the elementwise multiplication and square-root operations. Denoting  $g_k = \nabla f(x^k, s_k)$ , for Adam we choose

$$v_k = (1 - \beta_2)v_{k-1} + \beta_2(g_k \odot g_k),$$

$$\mathbf{D}_k = \text{Diag}(\epsilon \mathbf{1}_d + \sqrt{v_k / (1 - \beta_2^k)}),$$

where  $\beta_2 \in [0, 1)$ ,  $\epsilon > 0$ . Using this preconditioner with Lemma 3.1 gives Algorithm 2, called MoMo-Adam. Note that here we choose  $\rho_{j,k} = (1 - \beta)\beta^{k-j}$  (cf. Section 2.3) which gives the standard averaging scheme of Adam. We focus on MoMo versions of SGD-M and Adam because these are the two most widely used methods. However, from Lemma 3.1 we could easily obtain a MoMo-version any other preconditioned momentum method (e.g. Adabelief (Zhuang et al., 2020)).

## 4. Estimating a Lower Bound

So far, we have assumed that the lower-bound estimates  $(f_*^k)$  are given with  $f_*^k = 0$  being the default. However, this might not be a tight estimate of  $f^*$  (e.g. when training transformers). In such situations, we derive an online estimate of the lower bound. In particular, for convex functions we will derive a lower bound for an unbiased estimate of  $f(x^*)$  given by

$$\bar{f}_*^k := \frac{1}{\rho_k} \sum_{j=1}^k \rho_{j,k} f(x^*, s_j). \quad (17)$$

Though  $\bar{f}_*^k$  is not equal to  $f(x^*)$ , it is an unbiased estimate since  $\mathbb{E}[f(x^*, s_j)] = f(x^*)$  and hence  $\mathbb{E}[\bar{f}_*^k] = f(x^*)$ . It is also a reasonable choice since we motivated our method

using the analogous approximation of  $f(x)$  in (5). The following lemma derives an estimate  $f_*^k \geq 0$  for  $\bar{f}_*$  given in (17) by using readily available information for any momentum-based method, such as Algorithm 2.

**Lemma 4.1.** Let  $f(x, s)$  be convex in  $x$  for all  $s \in \mathcal{D}$ . Consider the iterates  $x^{k+1} = x^k - \tau_k \mathbf{D}_k^{-1} d_k$  for  $\tau_k > 0$ . Let

$$\eta_k := \prod_{j=2}^k \lambda_{\min}(\mathbf{D}_j^{-1} \mathbf{D}_{j-1})$$

$$h_k := \bar{f}_k + \langle d_k, x^k \rangle - \gamma_k.$$

It follows that  $\bar{f}_*^k \geq f_*^{k+1}$  where

$$f_*^{k+1} := \frac{1}{2\eta_k \tau_k \rho_k} \left( \sum_{j=1}^k 2\eta_j \tau_j (h_j - \frac{1}{2} \tau_j \|d_j\|_{\mathbf{D}_j^{-1}}^2) - D_1^2 - 2 \sum_{j=1}^{k-1} \eta_j \tau_j \rho_j \bar{f}_*^j \right)$$

where  $D_1 := \|x^1 - x^*\|_{\mathbf{D}_1}$ . Bootstrapping by using  $f_*^k \approx \bar{f}_*^{k-1}$  we have for  $k \geq 2$  that

$$f_*^{k+1} \approx \frac{1}{\rho_k} \left( h_k - \frac{1}{2} \tau_k \|d_k\|_{\mathbf{D}_k^{-1}}^2 \right). \quad (18)$$

To simplify the discussion, consider the case without a preconditioner, i.e.  $\mathbf{D}_k = \mathbf{Id}$ , thus  $\eta_k = 1$ . Note that  $f_*^{k+1}$  depends on the initial distance to the solution  $D_1$ , which we do not know. Fortunately,  $D_1$  does not appear in the bootstrapped update (18), because it only appears in  $f_*^1$ . We can circumvent this initial dependency by setting  $f_*^1 = 0$ .

We can now introduce MoMo or MoMo-Adam with  $f_*^k$  estimated as in (18), which we call MoMo\* and MoMo-Adam\*. We need one more precautionary measure: we want to avoid that the step size  $\tau_k$  in (15) becomes zero, which occurs if

$$(1 + \alpha_k \lambda) \rho_k f_*^k \geq (1 + \alpha_k \lambda) (\bar{f}_k - \gamma_k) + \langle d_k, x^k \rangle =: h_k^\lambda. \quad (19)$$

Hence, in each iteration of MoMo\* or MoMo-Adam\*, we call the `ResetStar` routine in Algorithm 3 *before* the update of  $x^{k+1}$  that checks if this upper bound has been crossed, and if so, resets  $f_*^k$  to be sufficiently small. After updating  $x^{k+1}$ , we update  $f_*^{k+1}$  with `EstimateStar` routine in Algorithm 4, according to Lemma 4.1. The full algorithm of MoMo\* is given in Algorithm 6 in the Appendix. We give an example of how the values of  $f_*^k$  converge to  $f_*$  in Appendix F.5.

## 5. Convergence Analysis

Here we will show that MoMo attains a  $\mathcal{O}(1/\sqrt{K})$  rate for convex problems with interpolation. First, if  $f_*^k = \bar{f}_*^k$  where  $\bar{f}_*^k$  is (17), the next lemma shows that for any preconditioner

---

### Algorithm 3 `ResetStar`

---

**Input:**  $f_*^k, \alpha_k, \lambda, \rho_k, h_k^\lambda$   
**if** (19) **then**  
 $f_*^k = \max \left\{ \frac{1}{2} [(1 + \alpha_k \lambda) \rho_k]^{-1} h_k^\lambda, f_*^1 \right\}$   
**end if**  
**Return**  $f_*^k$

---



---

### Algorithm 4 `EstimateStar`

---

**Input:**  $\bar{f}_k, x^k, \gamma_k, \tau_k, d_k, \mathbf{D}_k, \rho_k$   
 $h_k = \bar{f}_k + \langle d_k, x^k \rangle - \gamma_k$   
 $f_*^{k+1} = \max \left\{ \rho_k^{-1} (h_k - \frac{1}{2} \tau_k \|d_k\|_{\mathbf{D}_k^{-1}}^2), f_*^1 \right\}$   
**Return**  $f_*^{k+1}$

---

and convex loss, the iterates of MoMo do not increase the distance to a given optimal point in each step.

**Lemma 5.1.** Let  $f(\cdot, s)$  be convex for every  $s$  and let  $x^* \in \arg \min_{x \in \mathbb{R}^d} f(x)$ . For the iterates of the general MoMo update (cf. Lemma 3.1) with  $\lambda = 0$  and  $f_*^k = \bar{f}_*^k$ , it holds

$$\|x^{k+1} - x^*\|_{\mathbf{D}_k}^2 \leq \|x^k - x^*\|_{\mathbf{D}_k}^2 - \tau_k (h_k - \rho_k \bar{f}_*^k)_+. \quad (20)$$

This monotonicity property is already remarkable as it does not hold in general for standard SGD (Garrigos & Gower, 2023). In the following theorem, we will use it to prove convergence of MoMo (Algorithm 1) for the convex case under interpolation, that is, assuming

$$f(x^*, s) = \inf_x f(x, s) = f_* \quad \text{for all } s \in \mathcal{D}. \quad (21)$$

Interpolation holds when there exists model parameters  $x^*$  such that the loss attains its infimum on every data point. Typically this occurs when the loss is zero for every data point.

**Theorem 5.2.** Let  $f(\cdot, s)$  be convex for every  $s$  and let  $x^* \in \arg \min_{x \in \mathbb{R}^d} f(x)$ . Assume that (21) holds. Let  $(x^k)$  be the iterates of Algorithm 1 with  $f_*^k = f_*$ ,  $\alpha_k = +\infty$  for all  $k \in \mathbb{N}$  and assume that  $d_k \neq 0$  for all  $k \in \mathbb{N}$ . Define

$$B := \{x \mid \|x - x^*\| \leq \|x^1 - x^*\|\}.$$

Assume that there exists  $G > 0$  such that  $\max_{x \in B} \mathbb{E} [\|\nabla f(x, s)\|^2] = G^2 < \infty$ . Then, it holds

$$\min_{k=1, \dots, K} \mathbb{E} [f(x^k) - f_*] \leq \frac{G \|x^1 - x^*\|}{\sqrt{K} (1 - \beta)}.$$

We remark that Theorem 5.2 is an unusual result, since in the non-smooth setting for SGD, one needs to assume that

the gradients are *globally* bounded, that is, the function is globally Lipschitz continuous (Garrigos & Gower, 2023, Thm. 9.7) (alternatively, one can assume a bounded domain (Orabona, 2019)). Second, the step size to obtain the best iteration complexity requires knowledge of the global Lipschitz constant, and an upper bound of the initial distance to the solution  $\|x^0 - x^*\| \leq R$ . Both of the above is true as well for the analysis of SGD-M (Defazio & Gower, 2021, Thm. 10). For Theorem 5.2, we require neither of the two, but instead rely on interpolation and the mild assumption that the gradients are bounded *on the compact set*  $B$  and in expectation.

## 6. Experiments

Our experiments will focus on the sensitivity with respect to choice of the learning rate  $\alpha_k$ . Schmidt et al. (2021) showed that most optimization methods perform equally well when being tuned. For practical use, a tuning budget needs to be considered; hence we are interested in methods that require little or no tuning. Here we investigate how using our MoMo adaptive learning rate can improve the stability of both SGD-M and Adam. To do this, for each task and model, we do a learning-rate sweep for both SGD-M, Adam, MoMo and MoMo-Adam and compare the resulting validation score for each learning rate.

For MoMo and MoMo-Adam, note that the effective step size (cf. (15)) has the form  $\tau_k = \min\{\frac{\alpha_k}{\rho_k}, \zeta_k\}$  with

$$\zeta_k := \frac{((1 + \alpha_k \lambda)(\bar{f}_k - \rho_k f_*^k - \gamma_k) + \langle d_k, x^k \rangle)_+}{\|d_k\|_{\mathbf{D}_k^{-1}}^2}. \quad (22)$$

We refer to Algorithm 1, line 9 and Algorithm 2, line 12 for the exact formula for MoMo and MoMo-Adam (For MoMo we have that  $\rho_k = 1, \mathbf{D}_k = \mathbf{Id}$ ). We will refer to  $\alpha_k$  as the (*user-specified*) learning rate and to  $\tau_k$  as the *adaptive learning rate*.

### 6.1. Zero as Lower Bound

#### 6.1.1. CONSTANT LEARNING RATE

First, we compare the MoMo methods to SGD-M and Adam for problems where zero is a good estimate of the optimal value  $f^*$ . In this section, we set  $f_*^k = 0$  for all  $k \in \mathbb{N}$  for MoMo(-Adam).

**Models and Datasets.** Here we consider the tasks (additional details in Appendix F.3):

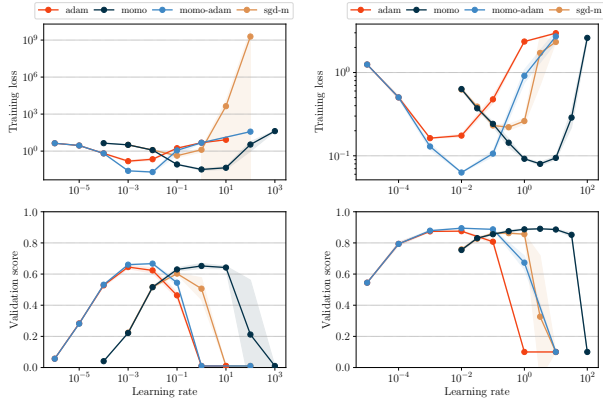
- ResNet110 for CIFAR100, ResNet20, VGG16, and ViT for CIFAR10
- DLRM for Criteo Display Advertising Challenge,
- MLP for MNIST: two hidden layers (size 100) and ReLU.

**Parameter Settings.** We use default choices for momentum parameter  $\beta = 0.9$  for MoMo and SGD-M, and  $(\beta_1, \beta_2) = (0.9, 0.999)$  for MoMo-Adam and Adam respectively. In the experiments of this section, we always report averaged values over three seeds (five for DLRM), and do not use weight decay ( $\lambda = 0$ ).

**Discussion.** We run MoMo, MoMo-Adam, Adam and SGD-M, for a fixed number of epochs (cf. Appendix F.3), using a constant learning rate  $\alpha_k = \alpha_0$ . The plots in Figure 2 show the final training loss and validation set accuracy of each method when varying the learning rate  $\alpha_0$ . The training curves for the best runs can be found in Figures F.1 and F.2. For VGG16 and ViT for CIFAR10 and MLP for MNIST, the same plots can be found in Appendix F. We observe that for small learning rates MoMo (MoMo-Adam) is identical to SGD-M (Adam). This is expected, since for small  $\alpha_0$ , we have  $\tau_k = \alpha_0$  (see (15)).

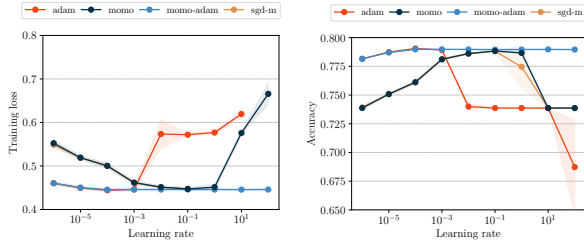
For larger learning rates, we see that MoMo and MoMo-Adam improve the training loss and validation accuracy, but SGD-M and Adam decline in performance or fail to converge. Most importantly, MoMo(-Adam) consistently extends the range of “good” learning rates by over one order of magnitude. Further, MoMo(-Adam) achieve the overall best validation accuracy for all problems except DLRM and ViT, where the gap to the best score is minute and within the standard deviation of running multiple seeds (see Table 1).

This advantage can be explained with the adaptivity of the step size of MoMo(-Adam). In Figure F.4a, we plot the adaptive term  $\zeta_k$  (22) for MoMo on a ResNet20. For  $\alpha_0 \in [1, 10]$ , we observe that the effective learning rate  $\tau_k$  is adaptive even though  $\alpha_k$  is constant. We observe two phenomena: firstly, in Figure F.4a MoMo is doing an automatic learning rate decay *without any user choice for a learning-rate schedule*. Secondly, in the very first iterations, MoMo is doing a warm-up of the learning rate as  $\tau_k = \zeta_k$  starts very small, but quickly becomes large. Both dynamics of  $\tau_k$  seemingly improve performance and stability. We also observe faster initial training progress of MoMo(-Adam) (cf. Figures F.1 and F.2). We provide additional comparisons to Adabelief (Zhuang et al., 2020), Adabound (Luo et al., 2019), and Lion (Chen et al., 2023) in Figure F.6 in the Appendix. While MoMo(-Adam) performs favourably in this additional benchmark, we stress that it would be easy to derive a MoMo version of any preconditioned momentum method (such as Adabelief or Adabound). Figure F.6 also shows the advantage of MoMo when comparing to SGD-M with exponentially decaying schedule for  $\alpha_k$  on the CIFAR100 experiment.



(a) ResNet110 for CIFAR100

(b) ResNet20 for CIFAR10



(c) DLRM for Criteo

Figure 2. Training loss and validation accuracy after a fixed number of epochs, for varying (constant) learning rate  $\alpha_0$ . Shaded area depicts two standard deviations.

### 6.1.2. USING A LEARNING-RATE SCHEDULE

Here we present results for training a vision transformer (ViT) on Imagenet-1k (Figure 3), and a diffusion model (UNet architecture) on the Smithsonian Butterflies.

Here we only compare MoMo-Adam to AdamW. This is in order to keep the computational expense within reasonable limits and because Adam is the prevalent method for these tasks. Experiment details are provided in Appendix F.3.

What distinguishes these experiments to previous ones, is that we use MoMo-Adam and AdamW with a learning-rate schedule for  $\alpha_k$ . For both tasks, it is standard practice to use a warmup (from a very small value to a specified base value  $\alpha_{\text{base}}$ ) followed by cosine decay (Dosovitskiy et al., 2021). We sweep over  $\alpha_{\text{base}}$  and investigate again sensitivity with respect to this choice. From Figure 3, for the ViT training, we see that MoMo-Adam (i) works on a larger range of base learning-rate values and (ii) reaches a higher accuracy for the best value of  $\alpha_{\text{base}}$  (here 0.01).

The results for the diffusion model are similar and presented in Figures F.7 and F.8 in the Appendix. To summarize, we reach the same conclusion as previously: MoMo-Adam is easier to tune as it works for a wider range of learning rates, stabilizes training, and it can improve the best accuracy.

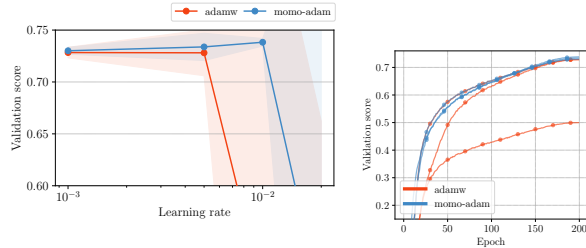


Figure 3. ViT for Imagenet-1k. Left: Final validation set accuracy (top-1) for different learning-rate values  $\alpha_{\text{base}}$ . Right: Training curves for the three best values of  $\alpha_{\text{base}}$  for both methods.

For all of the above tasks, the (training) loss converges to values below 0.5. Next, we consider two problems where the final training loss is significantly above zero. In such situations, we find that the MoMo methods with  $f_*^k = 0$  are less likely to make use of the adaptive term  $\zeta_k$ . As a consequence, MoMo with  $f_*^k = 0$  will yield little or no improvement. To see improvement, we employ the online estimation of a lower bound for MoMo given in Lemma 4.1.

### 6.2. Online Lower Bound Estimation

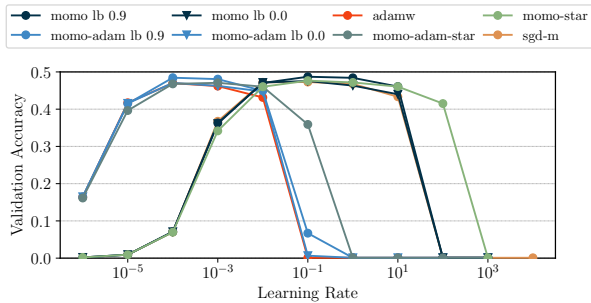
We now consider image classification on Imagenet32/-1k and a transformer for German-to-English translation. For both problems, the optimal value  $f^*$  is far away from zero and hence we use MoMo with a known estimate of  $f^*$  or with the online estimation developed in Section 4. Details on models and datasets are listed in Appendix F.3.

**Imagenet.** We train a ResNet18 for Imagenet32 and give the resulting validation accuracy in Figure 4a for weight decay  $\lambda = 0$ . We show results for  $\lambda = 10^{-4}$  and for Imagenet-1k in the Appendix in Figure F.5. We run MoMo(-Adam) first with constant lower bound  $f_*^k = 0$  and an oracle value  $f_*^k = 0.9$ . Further, we run MoMo(-Adam)\* (indicated by the suffix *-star* in the plots), (cf. Algorithm 6). We compare to SGD-M and AdamW. For all methods, we use a constant learning rate  $\alpha_k = \alpha_0$  and vary the value of  $\alpha_0$ .

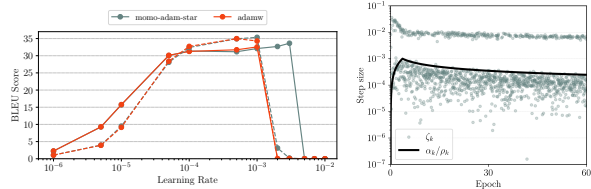
First we observe in Figure 4a that setting  $f_*^k = 0$  leads to similar performance as the baseline method (in particular it is never worse). Next, observe that the tighter lower bound  $f_*^k = 0.9$  leads to improvement for all learning rates. Finally, the online estimated lower bound widens the range of learning rate with good accuracy by an order of magnitude and leads to small improvements in top accuracy.

**Transformer for German-to-English Translation.** We consider the task of neural machine translation from German to English by training an encoder-decoder transformer architecture (Vaswani et al., 2017) on the IWSLT14 dataset. We run two settings, namely dropout of 0.1 and 0.3. We





(a) ResNet18 for Imagenet32



(b) Encoder-Decoder Transformer for IWSLT14

Figure 4. Validation accuracy over a range of learning rates  $\alpha_0$ . (a) Imagenet32 without weight decay ( $\lambda = 0$ ). (b) Left: IWSLT14 translation task with dropout 0.1 (plain) or 0.3 (dashed). Right: Learning rate schedule (black) and adaptive step sizes (grey dots) of MoMo-Adam\* for  $\alpha_{\text{base}} = 10^{-3}$ .

fine-tune the hyperparameters of the baseline AdamW: for the learning-rate schedule  $\alpha_k$ , we use a linear warm-up of 4000 iterations from zero to a given base value  $\alpha_{\text{base}}$  followed by an inverse square-root decay (cf. Figure 4b for an example curve and the adaptive step sizes). All other parameter settings are given in Appendix F.3. MoMo-Adam\* uses the same hyperparameter settings as AdamW.

Figure 4b shows the BLEU score after 60 epochs when varying the base learning rate  $\alpha_{\text{base}}$ : MoMo-Adam\* is on par or better than AdamW on the full range of initial learning rates and for both dropout values, with only a small improvement for larger values of  $\alpha_{\text{base}}$ . While this improvement is not as substantial as for previous examples, we remark that for this particular task we compare to a fine-tuned configuration of AdamW.

## 7. Conclusion

We present MoMo and MoMo-Adam, adaptive learning rates for SGD-M and Adam. The main conceptual insight is that momentum can be used to build a model of the loss by averaging a stream of loss function values and gradients. Combined with truncating this average at a known lower bound of the loss, we obtain the MoMo algorithms. This technique can be applied to all momentum type methods, including variants of Adam.

We show examples where incorporating MoMo into SGD-M

and Adam significantly reduces the sensitivity to learning rate choice. This can be particularly helpful for practitioners who look for good out-of-the-box optimization performance for new tasks.

## Acknowledgements

The computations in this work were, in part, run at facilities supported by the Scientific Computing Core at the Flatiron Institute, a division of the Simons Foundation.

All models and datasets for this project were utilized by authors at the Flatiron Institute and the Technical University of Munich.

## Impact Statement

This paper presents work whose goal is to advance the field of Machine Learning. There are many potential societal consequences of our work, none which we feel must be specifically highlighted here.

## References

Asi, H. and Duchi, J. C. Stochastic (approximate) proximal point methods: convergence, optimality, and adaptivity. *SIAM J. Optim.*, 29(3):2257–2290, 2019. ISSN 1052-6234. doi: 10.1137/18M1230323.

Berrada, L., Zisserman, A., and Kumar, M. P. Training neural networks for and by interpolation. In *Proceedings of the 37th International Conference on Machine Learning*, volume 119 of *Proceedings of Machine Learning Research*, pp. 799–809. PMLR, 13–18 Jul 2020.

Chadha, K., Cheng, G., and Duchi, J. C. Accelerated, optimal, and parallel: Some results on model-based stochastic optimization. January 2021.

Chen, K., Cutkosky, A., and Orabona, F. Implicit parameter-free online learning with truncated linear models. In Dasgupta, S. and Haghtalab, N. (eds.), *Proceedings of The 33rd International Conference on Algorithmic Learning Theory*, volume 167 of *Proceedings of Machine Learning Research*, pp. 148–175. PMLR, 29 Mar–01 Apr 2022. URL <https://proceedings.mlr.press/v167/chen22a.html>.

Chen, X., Liang, C., Huang, D., Real, E., Wang, K., Pham, H., Dong, X., Luong, T., Hsieh, C., Lu, Y., and Le, Q. V. Symbolic discovery of optimization algorithms. In Oh, A., Naumann, T., Globerson, A., Saenko, K., Hardt, M., and Levine, S. (eds.), *Advances in Neural Information Processing Systems 36: Annual Conference on Neural Information Processing Systems 2023, NeurIPS 2023, New Orleans, LA, USA, December 10 - 16, 2023*, 2023.

- Davis, D. and Drusvyatskiy, D. Stochastic model-based minimization of weakly convex functions. *SIAM J. Optim.*, 29(1):207–239, 2019. ISSN 1052-6234. doi: 10.1137/18M1178244.
- Defazio, A. and Gower, R. M. The power of factorial powers: New parameter settings for (stochastic) optimization. In Balasubramanian, V. N. and Tsang, I. (eds.), *Proceedings of The 13th Asian Conference on Machine Learning*, volume 157 of *Proceedings of Machine Learning Research*, pp. 49–64. PMLR, 17–19 Nov 2021. URL <https://proceedings.mlr.press/v157/defazio21a.html>.
- Defazio, A. and Mishchenko, K. Learning-rate-free learning by D-adaptation. In Krause, A., Brunskill, E., Cho, K., Engelhardt, B., Sabato, S., and Scarlett, J. (eds.), *Proceedings of the 40th International Conference on Machine Learning*, volume 202 of *Proceedings of Machine Learning Research*, pp. 7449–7479. PMLR, 23–29 Jul 2023a. URL <https://proceedings.mlr.press/v202/defazio23a.html>.
- Defazio, A. and Mishchenko, K. Learning-rate-free learning by D-Adaptation. In Krause, A., Brunskill, E., Cho, K., Engelhardt, B., Sabato, S., and Scarlett, J. (eds.), *Proceedings of the 40th International Conference on Machine Learning*, volume 202 of *Proceedings of Machine Learning Research*, pp. 7449–7479. PMLR, 23–29 Jul 2023b.
- Dosovitskiy, A., Beyer, L., Kolesnikov, A., Weissenborn, D., Zhai, X., Unterthiner, T., Dehghani, M., Minderer, M., Heigold, G., Gelly, S., Uszkoreit, J., and Houshy, N. An image is worth 16x16 words: Transformers for image recognition at scale. In *9th International Conference on Learning Representations, ICLR 2021, Virtual Event, Austria, May 3-7, 2021*. OpenReview.net, 2021. URL <https://openreview.net/forum?id=YicbFdNTTy>.
- Duchi, J., Hazan, E., and Singer, Y. Adaptive subgradient methods for online learning and stochastic optimization. *J. Mach. Learn. Res.*, 12:2121–2159, 2011. ISSN 1532-4435.
- Garrigos, G. and Gower, R. M. Handbook of convergence theorems for (stochastic) gradient methods, 2023.
- Gower, R., Sebbouh, O., and Loizou, N. SGD for structured nonconvex functions: Learning rates, minibatching and interpolation. In Banerjee, A. and Fukumizu, K. (eds.), *Proceedings of The 24th International Conference on Artificial Intelligence and Statistics*, volume 130 of *Proceedings of Machine Learning Research*, pp. 1315–1323. PMLR, 13–15 Apr 2021. URL <https://proceedings.mlr.press/v130/gower21a.html>.
- He, K., Zhang, X., Ren, S., and Sun, J. Deep residual learning for image recognition. In *2016 IEEE Conference on Computer Vision and Pattern Recognition (CVPR)*, pp. 770–778, 2016. doi: 10.1109/CVPR.2016.90.
- Kaplan, J., McCandlish, S., Henighan, T., Brown, T. B., Chess, B., Child, R., Gray, S., Radford, A., Wu, J., and Amodei, D. Scaling laws for neural language models. *CoRR*, abs/2001.08361, 2020. URL <https://arxiv.org/pdf/2001.08361.pdf>.
- Kingma, D. P. and Ba, J. Adam: A method for stochastic optimization. In Bengio, Y. and LeCun, Y. (eds.), *3rd International Conference on Learning Representations, ICLR 2015, San Diego, CA, USA, May 7-9, 2015, Conference Track Proceedings*, 2015.
- Krogh, A. and Hertz, J. A simple weight decay can improve generalization. In Moody, J., Hanson, S., and Lippmann, R. (eds.), *Advances in Neural Information Processing Systems*, volume 4. Morgan-Kaufmann, 1991. URL <https://proceedings.neurips.cc/paper/1991/file/8eefcfd5990e441f0fb6f3fad709e21-Paper.pdf>.
- Loizou, N., Vaswani, S., Hadj Laradji, I., and Lacoste-Julien, S. Stochastic Polyak step-size for SGD: An adaptive learning rate for fast convergence. In Banerjee, A. and Fukumizu, K. (eds.), *Proceedings of The 24th International Conference on Artificial Intelligence and Statistics*, volume 130 of *Proceedings of Machine Learning Research*, pp. 1306–1314. PMLR, 13–15 Apr 2021. URL <https://proceedings.mlr.press/v130/loizou21a.html>.
- Loshchilov, I. and Hutter, F. Decoupled weight decay regularization. In *7th International Conference on Learning Representations, ICLR 2019, New Orleans, LA, USA, May 6-9, 2019*. OpenReview.net, 2019. URL <https://openreview.net/forum?id=Bkg6RiCqY7>.
- Luo, L., Xiong, Y., Liu, Y., and Sun, X. Adaptive gradient methods with dynamic bound of learning rate. In *Proceedings of the 7th International Conference on Learning Representations*, May 2019.
- Ma, S., Bassily, R., and Belkin, M. The power of interpolation: Understanding the effectiveness of SGD in modern over-parametrized learning. In Dy, J. and Krause, A. (eds.), *Proceedings of the 35th International Conference on Machine Learning*, volume 80 of *Proceedings of Machine Learning Research*, pp. 3325–3334. PMLR, 10–15 Jul 2018. URL <https://proceedings.mlr.press/v80/ma18a.html>.
- Meng, S. Y. and Gower, R. M. A model-based method for minimizing CVaR and beyond. In Krause, A., Brunskill, E., Cho, K., Engelhardt, B., Sabato, S., and Scar-

- lett, J. (eds.), *Proceedings of the 40th International Conference on Machine Learning*, volume 202 of *Proceedings of Machine Learning Research*, pp. 24436–24456. PMLR, 23–29 Jul 2023. URL <https://proceedings.mlr.press/v202/meng23a.html>.
- Orabona, F. A modern introduction to online learning. *CoRR*, abs/1912.13213, 2019. URL <http://arxiv.org/abs/1912.13213>.
- Orabona, F. and Tommasi, T. Training deep networks without learning rates through coin betting. In Guyon, I., Luxburg, U. V., Bengio, S., Wallach, H., Fergus, R., Vishwanathan, S., and Garnett, R. (eds.), *Advances in Neural Information Processing Systems*, volume 30. Curran Associates, Inc., 2017.
- Orvieto, A., Lacoste-Julien, S., and Loizou, N. Dynamics of SGD with stochastic polyak stepsizes: Truly adaptive variants and convergence to exact solution. In *NeurIPS*, 2022.
- Ott, M., Edunov, S., Baevski, A., Fan, A., Gross, S., Ng, N., Grangier, D., and Auli, M. fairseq: A fast, extensible toolkit for sequence modeling. In *Proceedings of NAACL-HLT 2019: Demonstrations*, 2019.
- Paren, A., Berrada, L., Poudel, R. P. K., and Kumar, M. P. A stochastic bundle method for interpolation. *J Mach Learn Res*, 23(15):1–57, 2022. URL <http://jmlr.org/papers/v23/20-1248.html>.
- Polyak, B. T. Some methods of speeding up the convergence of iteration methods. *USSR Computational Mathematics and Mathematical Physics*, 4(5):1–17, 1964. ISSN 0041-5553.
- Polyak, B. T. *Introduction to optimization*. Translations Series in Mathematics and Engineering. Optimization Software, Inc., Publications Division, New York, 1987. ISBN 0-911575-14-6. Translated from the Russian, With a foreword by Dimitri P. Bertsekas.
- Raffel, C., Shazeer, N., Roberts, A., Lee, K., Narang, S., Matena, M., Zhou, Y., Li, W., and Liu, P. J. Exploring the limits of transfer learning with a unified text-to-text transformer. *J Mach Learn Res*, 21(140):1–67, 2020. URL <http://jmlr.org/papers/v21/20-074.html>.
- Robbins, H. and Monro, S. A stochastic approximation method. *Ann. Math. Statistics*, 22:400–407, 1951. ISSN 0003-4851. doi: 10.1214/aoms/1177729586.
- Ronneberger, O., Fischer, P., and Brox, T. U-net: Convolutional networks for biomedical image segmentation. In *Lecture Notes in Computer Science*, pp. 234–241. Springer International Publishing, 2015. doi: 10.1007/978-3-319-24574-4\_28.
- Schaipp, F., Gower, R. M., and Ulbrich, M. A stochastic proximal Polyak step size. *Transactions on Machine Learning Research*, 2023. ISSN 2835-8856. URL <https://openreview.net/forum?id=jWr41htaB3>. Reproducibility Certification.
- Schmidt, R. M., Schneider, F., and Hennig, P. Descending through a crowded valley - benchmarking deep learning optimizers. In Meila, M. and Zhang, T. (eds.), *Proceedings of the 38th International Conference on Machine Learning*, volume 139 of *Proceedings of Machine Learning Research*, pp. 9367–9376. PMLR, 18–24 Jul 2021. URL <https://proceedings.mlr.press/v139/schmidt21a.html>.
- Sebbouh, O., Gower, R. M., and Defazio, A. Almost sure convergence rates for stochastic gradient descent and stochastic heavy ball. In Belkin, M. and Kpotufe, S. (eds.), *Proceedings of Thirty Fourth Conference on Learning Theory*, volume 134 of *Proceedings of Machine Learning Research*, pp. 3935–3971. PMLR, 15–19 Aug 2021. URL <https://proceedings.mlr.press/v134/sebbouh21a.html>.
- Sharir, O., Peleg, B., and Shoham, Y. The cost of training NLP models: A concise overview, 2020.
- Simonyan, K. and Zisserman, A. Very deep convolutional networks for large-scale image recognition. In Bengio, Y. and LeCun, Y. (eds.), *3rd International Conference on Learning Representations, ICLR 2015, San Diego, CA, USA, May 7-9, 2015, Conference Track Proceedings*, 2015. URL <http://arxiv.org/abs/1409.1556>.
- Sun, R.-Y. Optimization for deep learning: An overview. *J. Oper. Res. Soc. China*, 8(2):249–294, jun 2020. doi: 10.1007/s40305-020-00309-6.
- Tien, J.-B. and Chapelle, O. Display advertising challenge, 2014. URL <https://kaggle.com/competitions/criteo-display-ad-challenge>.
- Vaswani, A., Shazeer, N., Parmar, N., Uszkoreit, J., Jones, L., Gomez, A. N., Kaiser, L., and Polosukhin, I. Attention is all you need. In Guyon, I., Luxburg, U. V., Bengio, S., Wallach, H., Fergus, R., Vishwanathan, S., and Garnett, R. (eds.), *Advances in Neural Information Processing Systems*, volume 30. Curran Associates, Inc., 2017. URL [https://proceedings.neurips.cc/paper\\_files/paper/2017/file/3f5ee243547dee91fbd053c1c4a845aa-Paper.pdf](https://proceedings.neurips.cc/paper_files/paper/2017/file/3f5ee243547dee91fbd053c1c4a845aa-Paper.pdf).
- Vaswani, S., Mishkin, A., Laradji, I. H., Schmidt, M., Gidel, G., and Lacoste-Julien, S. Painless stochastic gradient: Interpolation, line-search, and convergence rates. In *Advances in Neural Information Processing Systems 32: Annual Conference on Neural Information Processing*

*Systems 2019, NeurIPS 2019, December 8-14, 2019, Vancouver, BC, Canada*, pp. 3727–3740, 2019. URL <https://proceedings.neurips.cc/paper/2019/hash/2557911c1bf75c2b643afb4ecbfc8ec2-Abstract.html>.

Wang, X., Johansson, M., and Zhang, T. Generalized Polyak step size for first order optimization with momentum. In Krause, A., Brunskill, E., Cho, K., Engelhardt, B., Sabato, S., and Scarlett, J. (eds.), *Proceedings of the 40th International Conference on Machine Learning*, volume 202 of *Proceedings of Machine Learning Research*, pp. 35836–35863. PMLR, 23–29 Jul 2023. URL <https://proceedings.mlr.press/v202/wang231.html>.

Zhang, G., Wang, C., Xu, B., and Grosse, R. B. Three mechanisms of weight decay regularization. In *7th International Conference on Learning Representations, ICLR 2019, New Orleans, LA, USA, May 6-9, 2019*, 2019.

Zhuang, J., Tang, T., Ding, Y., Tatikonda, S., Dvornik, N. C., Papademetris, X., and Duncan, J. S. Adabelief optimizer: Adapting stepsizes by the belief in observed gradients. In Larochelle, H., Ranzato, M., Hadsell, R., Balcan, M., and Lin, H. (eds.), *Advances in Neural Information Processing Systems 33: Annual Conference on Neural Information Processing Systems 2020, NeurIPS 2020, December 6-12, 2020, virtual*, 2020. URL <https://proceedings.neurips.cc/paper/2020/hash/d9d4f495e875a2e075a1a4a6e1b9770f-Abstract.html>.

Zhuang, Z., Liu, M., Cutkosky, A., and Orabona, F. Understanding AdamW through proximal methods and scale-freeness. *Transactions on Machine Learning Research*, 2022. URL <https://openreview.net/forum?id=IKhEPWGdwK>.

## A. Implementation details

### A.1. Notes on the Averaging Coefficients

**Lemma A.1.** Let  $\beta \in [0, 1)$ . Let  $\rho_{1,1} = 1$ , and for  $k \geq 2$  let

$$\rho_{j,k} = \begin{cases} \beta \rho_{j,k-1}, & j \leq k-1, \\ 1 - \beta, & j = k. \end{cases}$$

Then,  $\sum_{j=1}^k \rho_{j,k} = 1$  holds for all  $k \in \mathbb{N}$ . Further, for an arbitrary sequence  $(u_j)_{j \in \mathbb{N}} \subset \mathbb{R}^m$ ,  $m \in \mathbb{N}$ , consider the weighted sum

$$\bar{u}_k := \sum_{j=1}^k \rho_{j,k} u_j.$$

Then, if  $\bar{u}_0 := u_1$  it holds  $\bar{u}_k = (1 - \beta)u_k + \beta\bar{u}_{k-1}$  for all  $k \in \mathbb{N}$ .

*Proof.* We prove that  $\sum_{j=1}^k \rho_{j,k} = 1$  holds for all  $k \in \mathbb{N}$  by induction. For the base case  $k = 1$ , we have  $\rho_{1,1} = 1$  by definition. Assuming that  $\sum_{j=1}^{k-1} \rho_{j,k-1} = 1$ , we have

$$\sum_{j=1}^k \rho_{j,k} = \rho_{k,k} + \sum_{j=1}^{k-1} \rho_{j,k} = 1 - \beta + \beta \sum_{j=1}^{k-1} \rho_{j,k-1} = 1 - \beta + \beta = 1.$$

Consequently, we have  $\bar{u}_1 = \rho_{1,1}u_1 = u_1$ , and for  $k \geq 2$ ,

$$\begin{aligned} \bar{u}_k &= \sum_{j=1}^k \rho_{j,k} u_j = (1 - \beta)u_k + \sum_{j=1}^{k-1} \beta \rho_{j,k-1} u_j = (1 - \beta)u_k + \beta \sum_{j=1}^{k-1} \rho_{j,k-1} u_j \\ &= (1 - \beta)u_k + \beta \bar{u}_{k-1}. \end{aligned}$$

□

For the choice of  $\rho_{j,k}$  in Lemma A.1, unrolling the recursion, for  $k \geq 2$  we obtain the explicit formula

$$\rho_{j,k} = \begin{cases} (1 - \beta)\beta^{k-j}, & j \geq 2 \\ \beta^{k-1}, & j = 1. \end{cases} \quad (23)$$

**Averaging with Bias Correction.** Choosing  $\rho_{j,k} = (1 - \beta)\beta^{k-j}$ , we have  $\rho_{j,k} = \beta \rho_{j,k-1}$ , and  $\rho_{k,k} = 1 - \beta$ . Hence, we can update  $\bar{f}_k = (1 - \beta)f(x^k, s_k) + \beta\bar{f}_{k-1}$  and analogously for  $d_k, \gamma_k$ . However, this choice does not satisfy  $\sum_{j=1}^k \rho_{j,k} = 1$ . Indeed using the geometric series gives

$$\rho_k = (1 - \beta) \sum_{j=0}^{k-1} \beta^j = 1 - \beta^k.$$

This fact motivates scaling by the factor of  $1 - \beta^k$  which was termed *debiasing* in Adam. This alternative averaging scheme leads to a variant of MoMo with bias correction, presented in Algorithm 5. As the two presented choices of  $\rho_{j,k}$  are very similar, we do not expect major differences in their performance (cf. Remark A.2).

**Remark A.2.** Algorithm 5 differs from Algorithm 1 only in two steps: first, the quantities  $\bar{f}_0, d_0, \gamma_0$  are initialized at zero. Secondly, we use  $\frac{\alpha_k}{1 - \beta^k}$  instead of  $\alpha_k$  and  $(1 - \beta^k)f_*^k$  instead of  $f_*^k$  in line (7). As  $\beta \in [0, 1)$ , for late iteration number  $k$ , we can expect that both methods behave very similarly.

---

**Algorithm 5** MoMo-Bias: Model-based Momentum with bias correction.

Defaults settings  $\beta = 0.9$ .

---

- 1: **Input:**  $x^1 \in \mathbb{R}^d$ ,  $\beta \in [0, 1)$ ,  $\alpha_k > 0$ ,  $(f_*^k)_{k \in \mathbb{N}} \subset \mathbb{R}$ .
  - 2: **Initialize:**  $\bar{f}_0 = 0$ ,  $d_0 = 0$  and  $\gamma_0 = 0$ .
  - 3: **for**  $k = 1$  **to**  $K - 1$  **do**
  - 4:    $\bar{f}_k = (1 - \beta)f(x^k, s_k) + \beta\bar{f}_{k-1}$
  - 5:    $d_k = (1 - \beta)\nabla f(x^k, s_k) + \beta d_{k-1}$
  - 6:    $\gamma_k = (1 - \beta)\langle \nabla f(x^k, s_k), x^k \rangle + \beta\gamma_{k-1}$
  - 7:    $x^{k+1} = x^k - \min \left\{ \frac{\alpha_k}{1 - \beta^k}, \frac{(\bar{f}_k - (1 - \beta^k)f_*^k + \langle d_k, x^k \rangle - \gamma_k)_+}{\|d_k\|^2} \right\} d_k$ .
  - 8: **end for**
- 

## A.2. Comparison of MoMo-Adam to AdamW

Algorithm 2 naturally compares to AdamW (Loshchilov & Hutter, 2019). Note that the update of AdamW (in the notation of Algorithm 2) can be written as

$$x^{k+1} = (1 - \alpha_k \lambda)x^k - \frac{\alpha_k}{1 - \beta_1^k} \mathbf{D}_k^{-1} d_k,$$

Compared to Algorithm 2, line 12, the weight decay of AdamW is not done dividing the whole expression by  $\frac{1}{1 + \alpha_k \lambda}$ , but instead multiplying only  $x^k$  with  $1 - \alpha_k \lambda$ . This is a first-order Taylor approximation (Zhuang et al., 2022): for  $\alpha$  small it holds  $\frac{1}{1 + \alpha \lambda} \approx 1 - \alpha \lambda$  and  $\frac{\alpha}{1 + \alpha \lambda} \approx \alpha$ . If we would want to adapt this approximation, we could replace line 12 with

$$x^{k+1} = (1 - \lambda \alpha_k)x^k - \min \left\{ \frac{\alpha_k}{1 - \beta_1^k}, \frac{((1 + \lambda \alpha_k)(\bar{f}_k - (1 - \beta_1^k)f_*^k - \gamma_k) + \langle d_k, x^k \rangle)_+}{\|d_k\|_{\mathbf{D}_k^{-1}}^2} \right\} \mathbf{D}_k^{-1} d_k. \quad (24)$$

However, the results of (Zhuang et al., 2022) suggest that this approximation has almost no impact on the empirical performance.

## A.3. MoMo\*

Here we give the complete pseudocode for MoMo\*, that is the MoMo method that uses the estimator for  $f_*^k$  given in Lemma 4.1.

---

**Algorithm 6** MoMo\*: Adaptive learning rates and online estimation of  $f^*$ .

---

- 1: **Input:**  $x^1 \in \mathbb{R}^d$ ,  $\beta \in [0, 1)$ ,  $\alpha_k > 0$ ,  $f_*^1 \subset \mathbb{R}$ .
  - 2: **Initialize:**  $\bar{f}_0 = f(x^1, s_1)$ ,  $d_0 = \nabla f(x^1, s_1)$  and  $\gamma_0 = \langle d_0, x^1 \rangle$
  - 3: **for**  $k = 1$  **to**  $K - 1$  **do**
  - 4:    $\bar{f}_k = (1 - \beta)f(x^k, s_k) + \beta\bar{f}_{k-1}$
  - 5:    $\gamma_k = (1 - \beta)\langle \nabla f(x^k, s_k), x^k \rangle + \beta\gamma_{k-1}$
  - 6:    $d_k = (1 - \beta)\nabla f(x^k, s_k) + \beta d_{k-1}$
  - 7:    $f_*^k = \text{ResetStar}()$
  - 8:    $x^{k+1} = x^k - \min \left\{ \alpha_k, \frac{(\bar{f}_k - f_*^k + \langle d_k, x^k \rangle - \gamma_k)_+}{\|d_k\|^2} \right\} d_k$
  - 9:    $f_*^{k+1} = \text{EstimateStar}()$ .
  - 10: **end for**
  - 11: **return**  $x^K$
-

## B. Auxiliary Lemmas

**Lemma B.1.** Let  $y_0, a \in \mathbb{R}^p$  with  $a \neq 0$  and  $c \in \mathbb{R}$ . Let  $\beta > 0$ . The solution to

$$y^+ = \arg \min_y \left( \underbrace{c + \langle a, y - y_0 \rangle}_=: h(y) \right)_+ + \frac{1}{2\beta} \|y - y_0\|^2 \quad (25)$$

is given by

$$y^+ = y_0 - \underbrace{\min \left\{ \beta, \frac{(c)_+}{\|a\|^2} \right\}}_{=: \tau} a.$$

Moreover we have  $h(y^+) = (c - \tau \|a\|^2)_+$  and

$$h(y^+) = c - \tau \|a\|^2, \quad \text{if } c \geq 0. \quad (26)$$

*Proof.* Clearly, the objective of (25) is strongly convex and therefore there exists a unique solution. The (necessary and sufficient) first-order optimality condition is given by

$$0 = ta + \beta^{-1}(y^+ - y_0), \quad t \in \partial(\cdot)_+(c + \langle a, y^+ - y_0 \rangle). \quad (27)$$

We distinguish three cases:

(P1) Suppose  $c < 0$ . Then,  $y_0$  satisfies (27) with  $t = 0$  and hence  $y^+ = y_0$ . In this case  $\tau = 0$  and  $h(y^+) = 0 = (c)_+$ .

(P2) Let  $\bar{y} := y_0 - \beta a$  and assume  $c + \langle a, \bar{y} - y_0 \rangle > 0 \iff c - \beta \|a\|^2 > 0 \iff \frac{c}{\|a\|^2} > \beta$ . Then  $\bar{y}$  satisfies (27) with  $t = 1$  and hence  $y^+ = \bar{y}$ . As  $\beta > 0$ , hence  $c > 0$  and  $\tau = \beta$ . As  $h(y^+) = c + \langle a, y^+ - y_0 \rangle = c - \beta \|a\|^2$ , equation (26) holds.

(P3) If neither  $c < 0$  nor  $\frac{c}{\|a\|^2} > \beta$  hold, then it must hold  $c + \langle a, y^+ - y_0 \rangle = 0$ . Then, the optimality condition is  $0 = ta + \beta^{-1}(y^+ - y_0)$  for some  $t \in [0, 1]$ . Hence,  $y^+ = y_0 - t\beta a$  and  $c + \langle a, y^+ - y_0 \rangle = c - t\beta \|a\|^2 = 0 \iff t = \frac{c}{\beta \|a\|^2}$ . As  $c \geq 0$  we have  $t \geq 0$  and  $\frac{c}{\|a\|^2} \leq \beta$  implies  $t \leq 1$ . Hence,  $\tau = \frac{c}{\|a\|^2}$  and  $c - \tau \|a\|^2 = c - c = 0$ , so (26) holds. □

**Lemma B.2.** Let  $y_0, a \in \mathbb{R}^p$  with  $a \neq 0$  and  $c \in \mathbb{R}$ . Let  $\mathbf{D} \in \mathbb{R}^{p \times p}$  be a symmetric, positive definite matrix. The solution to

$$y^+ = \operatorname{argmin}_{y \in \mathbb{R}^p} \left( \underbrace{c + \langle a, y - y_0 \rangle}_=: h(y) \right)_+ + \frac{1}{2\alpha} \|y - y_0\|_{\mathbf{D}}^2 + \frac{\lambda}{2} \|y\|_{\mathbf{D}}^2 \quad (28)$$

is given by

$$y^+ = \frac{1}{1 + \lambda\alpha} \left[ y_0 - \underbrace{\min \left\{ \alpha, \frac{((1 + \lambda\alpha)c - \lambda\alpha \langle a, y_0 \rangle)_+}{\|a\|_{\mathbf{D}^{-1}}^2} \right\}}_{=: \tau} \right] \mathbf{D}^{-1} a.$$

Furthermore

$$h(y^+) = \left( c - \frac{\lambda\alpha}{1 + \lambda\alpha} \langle a, y_0 \rangle - \frac{\tau}{1 + \lambda\alpha} \|a\|_{\mathbf{D}^{-1}}^2 \right)_+.$$

*Proof.* First we complete the squares as follows

$$\begin{aligned} \frac{\lambda}{2} \|y\|_{\mathbf{D}}^2 + \frac{1}{2\alpha} \|y - y_0\|_{\mathbf{D}}^2 &= \frac{1}{2\alpha} \|y\|_{(1+\lambda\alpha)\mathbf{D}}^2 - \frac{1}{\alpha} \langle y, \mathbf{D}y_0 \rangle + \text{cst.}(y) \\ &= \frac{1}{2\alpha} \|y\|_{(1+\lambda\alpha)\mathbf{D}}^2 - \frac{1}{\alpha} \langle y, (1+\lambda\alpha)\mathbf{D}\frac{y_0}{1+\lambda\alpha} \rangle + \text{cst.}(y) \\ &= \frac{1}{2\alpha} \|y - \frac{1}{1+\lambda\alpha}y_0\|_{(1+\lambda\alpha)\mathbf{D}}^2 + \text{cst.}(y), \end{aligned}$$

where  $\text{cst.}(y)$  denotes terms that are constant in  $y$ . Using the above, (28) is equivalent to

$$\begin{aligned} y^+ &= \operatorname{argmin}_{y \in \mathbb{R}^p} h(y) + \frac{1}{2\alpha} \|y - \frac{1}{1+\lambda\alpha}y_0\|_{(1+\lambda\alpha)\mathbf{D}}^2 \\ &= \operatorname{argmin}_{y \in \mathbb{R}^p} \left( c + \langle a, y - \frac{1}{1+\lambda\alpha}y_0 \rangle + \left( \frac{1}{1+\lambda\alpha} - 1 \right) \langle a, y_0 \rangle \right)_+ + \frac{1}{2\alpha} \|y - \frac{1}{1+\lambda\alpha}y_0\|_{(1+\lambda\alpha)\mathbf{D}}^2. \end{aligned}$$

Let  $\hat{c} := c + \left( \frac{1}{1+\lambda\alpha} - 1 \right) \langle a, y_0 \rangle = c - \frac{\lambda\alpha}{1+\lambda\alpha} \langle a, y_0 \rangle$ . With this definition, problem (28) is equivalent to

$$y^+ = \operatorname{argmin}_{y \in \mathbb{R}^p} \left( \hat{c} + \langle a, y - \frac{1}{1+\lambda\alpha}y_0 \rangle \right)_+ + \frac{1}{2\alpha} \|y - \frac{1}{1+\lambda\alpha}y_0\|_{(1+\lambda\alpha)\mathbf{D}}^2.$$

Changing variables with  $z^+ = \mathbf{D}^{1/2}y^+$ ,  $z = \mathbf{D}^{1/2}y$ , and  $z_0 = \mathbf{D}^{1/2}y_0$  gives

$$z^+ = \operatorname{argmin}_{z \in \mathbb{R}^p} \left( \hat{c} + \langle \mathbf{D}^{-1/2}a, z - \frac{1}{1+\lambda\alpha}z_0 \rangle \right)_+ + \frac{(1+\lambda\alpha)}{2\alpha} \|z - \frac{1}{1+\lambda\alpha}z_0\|^2.$$

Applying Lemma B.1 with  $y_0 \leftarrow \frac{1}{1+\lambda\alpha}z_0$ ,  $c \leftarrow \hat{c}$ ,  $a \leftarrow \mathbf{D}^{-1/2}a$ ,  $\beta \leftarrow \frac{\alpha}{1+\lambda\alpha}$  gives

$$z^+ = \frac{1}{1+\lambda\alpha}z_0 - \min \left\{ \frac{\alpha}{1+\lambda\alpha}, \frac{(\hat{c})_+}{\|a\|_{\mathbf{D}^{-1}}^2} \right\} \mathbf{D}^{-1/2}a.$$

Changing variables back using  $y^+ = \mathbf{D}^{-1/2}z^+$ , substituting  $\hat{c} = c - \frac{\lambda\alpha}{1+\lambda\alpha} \langle a, y_0 \rangle$  and re-arranging the above gives

$$\begin{aligned} y^+ &= \frac{1}{1+\lambda\alpha}y_0 - \min \left\{ \frac{\alpha}{1+\lambda\alpha}, \frac{\left( c - \frac{\lambda\alpha}{1+\lambda\alpha} \langle a, y_0 \rangle \right)_+}{\|a\|_{\mathbf{D}^{-1}}^2} \right\} \mathbf{D}^{-1}a \\ &= \frac{1}{1+\lambda\alpha} \left[ y_0 - \min \left\{ \alpha, \frac{\left( (1+\lambda\alpha)c - \lambda\alpha \langle a, y_0 \rangle \right)_+}{\|a\|_{\mathbf{D}^{-1}}^2} \right\} \mathbf{D}^{-1}a \right]. \end{aligned} \tag{29}$$

□

## C. Missing Proofs

### C.1. Proof of Lemma 2.1

**Lemma 2.1.** [MoMo update] Let

$$\begin{aligned} d_k &:= \sum_{j=1}^k \rho_{j,k} \nabla f(x^j, s_j), \\ \bar{f}_k &:= \sum_{j=1}^k \rho_{j,k} f(x^j, s_j), \\ \gamma_k &:= \sum_{j=1}^k \rho_{j,k} \langle \nabla f(x^j, s_j), x^j \rangle. \end{aligned} \tag{11}$$



Using model (9), the closed form solution to (10) is

$$\begin{aligned} \tau_k &:= \min \left\{ \frac{\alpha_k}{\rho_k}, \frac{(\bar{f}_k + \langle d_k, x^k \rangle - \gamma_k - \rho_k f_*^k)_+}{\|d_k\|^2} \right\}, \\ x^{k+1} &= x^k - \tau_k d_k. \end{aligned} \quad (12)$$

*Proof.* Recall problem (10) given by

$$x^{k+1} = \operatorname{argmin}_{y \in \mathbb{R}^d} m_k(y) + \frac{1}{2\alpha_k} \|y - x^k\|^2.$$

Introducing

$$h_k := \sum_{j=1}^k \rho_{j,k} [f(x^j, s_j) + \langle \nabla f(x^j, s_j), x^k - x^j \rangle] = \bar{f}_k + \langle d_k, x^k \rangle - \gamma_k, \quad (30)$$

we have that

$$m_k(y) = \max \left\{ \rho_k^{-1} (h_k + \langle d_k, y - x^k \rangle), f_*^k \right\} = \left( \rho_k^{-1} (h_k + \langle d_k, y - x^k \rangle) - f_*^k \right)_+ + f_*^k. \quad (31)$$

Using (31), dropping the constant term  $f_*^k$ , and multiplying with  $\rho_k$ , problem (10) is equivalent to

$$x^{k+1} = \operatorname{argmin}_{y \in \mathbb{R}^d} \left( h_k + \langle d_k, y - x^k \rangle - \rho_k f_*^k \right)_+ + \frac{\rho_k}{2\alpha_k} \|y - x^k\|^2.$$

Applying Lemma B.1 with  $\beta \leftarrow \rho_k^{-1} \alpha_k$ ,  $c \leftarrow h_k - \rho_k f_*^k$ ,  $a \leftarrow d_k$  and  $y_0 \leftarrow x^k$  gives the result.  $\square$

## C.2. Proof of Lemma 3.1

**Lemma 3.1.** Using model (9), the closed form solution to (14) is given by

$$\tau_k = \min \left\{ \frac{\alpha_k}{\rho_k}, \frac{((1+\alpha_k \lambda)(\bar{f}_k - \rho_k f_*^k - \gamma_k) + \langle d_k, x^k \rangle)_+}{\|d_k\|_{\mathbf{D}_k^{-1}}^2} \right\}, \quad (15)$$

$$x^{k+1} = \frac{1}{1+\alpha_k \lambda} \left[ x^k - \tau_k \mathbf{D}_k^{-1} d_k \right]. \quad (16)$$

*Proof.* Recall problem (14) given by

$$x^{k+1} = \operatorname{argmin}_{y \in \mathbb{R}^d} m_k(y) + \frac{1}{2\alpha_k} \|y - x^k\|_{\mathbf{D}_k}^2 + \frac{\lambda}{2} \|y\|_{\mathbf{D}_k}^2.$$

We use again (31). Dropping the constant term  $f_*^k$ , and multiplying with  $\rho_k$ , problem (14) is equivalent to

$$x^{k+1} = \operatorname{argmin}_{y \in \mathbb{R}^d} \left( h_k + \langle d_k, y - x^k \rangle - \rho_k f_*^k \right)_+ + \frac{\rho_k}{2\alpha_k} \|y - x^k\|_{\mathbf{D}_k}^2 + \frac{\rho_k \lambda}{2} \|y\|_{\mathbf{D}_k}^2.$$

Now applying Lemma B.2 with  $y_0 \leftarrow x^k$ ,  $a \leftarrow d_k$ ,  $c \leftarrow h_k - \rho_k f_*^k$ ,  $\lambda \leftarrow \rho_k \lambda$ ,  $\alpha \leftarrow \rho_k^{-1} \alpha_k$  and  $\mathbf{D} \leftarrow \mathbf{D}_k$ , we obtain the result.  $\square$

## D. Estimating a Lower Bound: Proofs and Alternatives

### D.1. Proof of Lemma 4.1

**Lemma 4.1.** Let  $f(x, s)$  be convex in  $x$  for all  $s \in \mathcal{D}$ . Consider the iterates  $x^{k+1} = x^k - \tau_k \mathbf{D}_k^{-1} d_k$  for  $\tau_k > 0$ . Let

$$\begin{aligned}\eta_k &:= \prod_{j=2}^k \lambda_{\min}(\mathbf{D}_j^{-1} \mathbf{D}_{j-1}) \\ h_k &:= \bar{f}_k + \langle d_k, x^k \rangle - \gamma_k.\end{aligned}$$

It follows that  $\bar{f}_*^k \geq f_*^{k+1}$  where

$$\begin{aligned}f_*^{k+1} &:= \frac{1}{2\eta_k \tau_k \rho_k} \left( \sum_{j=1}^k 2\eta_j \tau_j (h_j - \frac{1}{2} \tau_j \|d_j\|_{\mathbf{D}_j^{-1}}^2) \right. \\ &\quad \left. - D_1^2 - 2 \sum_{j=1}^{k-1} \eta_j \tau_j \rho_j \bar{f}_*^j \right)\end{aligned}$$

where  $D_1 := \|x^1 - x^*\|_{\mathbf{D}_1}$ . Bootstrapping by using  $f_*^k \approx \bar{f}_*^{k-1}$  we have for  $k \geq 2$  that

$$f_*^{k+1} \approx \frac{1}{\rho_k} \left( h_k - \frac{1}{2} \tau_k \|d_k\|_{\mathbf{D}_k^{-1}}^2 \right). \quad (18)$$

*Proof.* Switching the index  $k \rightarrow j$  in the update rule, we have

$$x^{j+1} = x^j - \tau_j \mathbf{D}_j^{-1} d_j,$$

where  $\tau_j$  is the step size. Subtracting  $x^*$  from both sides, taking norms and expanding the squares we have that

$$\|x^{j+1} - x^*\|_{\mathbf{D}_j}^2 = \|x^j - x^*\|_{\mathbf{D}_j}^2 - 2\tau_j \langle d_j, x^j - x^* \rangle + \tau_j^2 \|d_j\|_{\mathbf{D}_j^{-1}}^2. \quad (32)$$

Now let  $\delta_{j+1} := \lambda_{\min}(\mathbf{D}_{j+1}^{-1} \mathbf{D}_j)$  and note that for every vector  $v \in \mathbb{R}^d$  we have that

$$\delta_{j+1} \|v\|_{\mathbf{D}_{j+1}}^2 \leq \|v\|_{\mathbf{D}_j}^2. \quad (33)$$

Indeed this follows since

$$\begin{aligned}\|v\|_{\mathbf{D}_j}^2 &= v^\top \mathbf{D}_j v = v^\top \mathbf{D}_{j+1}^{1/2} (\mathbf{D}_{j+1}^{-1/2} \mathbf{D}_j \mathbf{D}_{j+1}^{-1/2}) \mathbf{D}_{j+1}^{1/2} v \\ &\geq \lambda_{\min}(\mathbf{D}_{j+1}^{-1} \mathbf{D}_j) \|v\|_{\mathbf{D}_{j+1}}^2 = \delta_{j+1} \|v\|_{\mathbf{D}_{j+1}}^2.\end{aligned}$$

For simplicity, denote  $\nabla f_l = \nabla f(x^l, s_l)$ ,  $f_l = f(x^l, s_l)$ . We have that

$$\begin{aligned}\langle d_j, x^j - x^* \rangle &= \sum_{l=1}^j \rho_{l,j} \langle \nabla f_l, x^j - x^* \rangle \\ &= \sum_{l=1}^j \rho_{l,j} (\langle \nabla f_l, x^j - x^l \rangle + \langle \nabla f_l, x^l - x^* \rangle) \\ &\geq \sum_{l=1}^j \rho_{l,j} (\langle \nabla f_l, x^j - x^l \rangle + f_l - f(x^*, s_l)) \quad (\text{by convexity of } f(\cdot, s)) \\ &= \bar{f}_j + \langle d_j, x^j \rangle - \gamma_j - \sum_{l=1}^j \rho_{l,j} f(x^*, s_l) = h_j - \rho_j \bar{f}_*^j.\end{aligned} \quad (34)$$

Using (33) together with (34) in (32) gives

$$\begin{aligned}
 \delta_{j+1} \|x^{j+1} - x^*\|_{\mathbf{D}_{j+1}}^2 &\leq \|x^{j+1} - x^*\|_{\mathbf{D}_j}^2 \\
 &= \|x^j - x^*\|_{\mathbf{D}_j}^2 - 2\tau_j \langle d_j, x^j - x^* \rangle + \tau_j^2 \|d_j\|_{\mathbf{D}_j^{-1}}^2 \\
 &\leq \|x^j - x^*\|_{\mathbf{D}_j}^2 - 2\tau_j (h_j - \rho_j \bar{f}_*^j) + \tau_j^2 \|d_j\|_{\mathbf{D}_j^{-1}}^2.
 \end{aligned} \tag{35}$$

Now we will perform a weighted telescoping. We will multiply the above by  $\eta_j > 0$  such that  $\delta_{j+1}\eta_j = \eta_{j+1}$ , thus  $\eta_j = \eta_1 \prod_{l=2}^j \delta_l$ . Thus multiplying through by  $\eta_j$  we have that

$$\eta_{j+1} \|x^{j+1} - x^*\|_{\mathbf{D}_{j+1}}^2 \leq \eta_j \|x^j - x^*\|_{\mathbf{D}_j}^2 - 2\eta_j \tau_j (h_j - \rho_j \bar{f}_*^j) + \eta_j \tau_j^2 \|d_j\|_{\mathbf{D}_j^{-1}}^2.$$

Summing up from  $j = 1, \dots, k$  and telescoping we have that

$$\begin{aligned}
 0 &\leq \eta_{k+1} \|x^{k+1} - x^*\|_{\mathbf{D}_{k+1}}^2 \\
 &\leq \eta_1 \|x^1 - x^*\|_{\mathbf{D}_1}^2 - 2 \sum_{j=1}^k \eta_j \tau_j (h_j - \rho_j \bar{f}_*^j) + \sum_{j=1}^k \eta_j \tau_j^2 \|d_j\|_{\mathbf{D}_j^{-1}}^2.
 \end{aligned} \tag{36}$$

Re-arranging the above, choosing  $\eta_1 = 1$  and isolating  $\bar{f}_*^k$  gives

$$2\eta_k \tau_k \rho_k \bar{f}_*^k \geq 2 \sum_{j=1}^k \eta_j \tau_j h_j - \|x^1 - x^*\|_{\mathbf{D}_1}^2 - \sum_{j=1}^k \eta_j \tau_j^2 \|d_j\|_{\mathbf{D}_j^{-1}}^2 - 2 \sum_{j=1}^{k-1} \eta_j \tau_j \rho_j \bar{f}_*^j.$$

Dividing through by  $2\eta_k \tau_k \rho_k$  gives the main result. Finally the recurrence follows since, for  $k \geq 2$  we have that

$$\begin{aligned}
 f_*^{k+1} &= \frac{2 \sum_{j=1}^k \eta_j \tau_j h_j - \|x^1 - x^*\|_{\mathbf{D}_1}^2 - \sum_{j=1}^k \eta_j \tau_j^2 \|d_j\|_{\mathbf{D}_j^{-1}}^2 - 2 \sum_{j=1}^{k-1} \eta_j \tau_j \rho_j \bar{f}_*^j}{2\eta_k \tau_k \rho_k} \\
 &= \frac{\eta_{k-1} \tau_{k-1} \rho_{k-1}}{\eta_k \tau_k \rho_k} \underbrace{\frac{2 \sum_{j=1}^{k-1} \eta_j \tau_j h_j - \|x^1 - x^*\|_{\mathbf{D}_1}^2 - \sum_{j=1}^{k-1} \eta_j \tau_j^2 \|d_j\|_{\mathbf{D}_j^{-1}}^2 - 2 \sum_{j=1}^{k-2} \eta_j \tau_j \rho_j \bar{f}_*^j}{2\eta_{k-1} \tau_{k-1} \rho_{k-1}}}_{= f_*^k} \\
 &\quad + \frac{\eta_{k-1} \tau_{k-1} \rho_{k-1}}{\eta_k \tau_k \rho_k} \frac{2\eta_k \tau_k h_k - \eta_k \tau_k^2 \|d_k\|_{\mathbf{D}_k^{-1}}^2 - 2\eta_{k-1} \tau_{k-1} \rho_{k-1} \bar{f}_*^{k-1}}{2\eta_{k-1} \tau_{k-1} \rho_{k-1}} \\
 &= \frac{2\eta_{k-1} \tau_{k-1} \rho_{k-1} (f_*^k - \bar{f}_*^{k-1}) - \eta_k \tau_k^2 \|d_k\|_{\mathbf{D}_k^{-1}}^2 + 2\eta_k \tau_k h_k}{2\eta_k \tau_k \rho_k}.
 \end{aligned}$$

Now bootstrapping by using  $f_*^k \approx \bar{f}_*^{k-1}$  gives the result.  $\square$

## D.2. The Max Lower Bound

Here we derive an alternative estimate for the lower bound that does not require bootstrapping, contrary to Lemma 4.1.

**Lemma D.1.** Let  $f(x, s)$  be convex in  $x$  for every sample  $s$ . Furthermore let  $x^* \in \operatorname{argmin}_{x \in \mathbb{R}^d} f(x)$ . Consider the iterates

$x^{k+1} = x^k - \tau_k \mathbf{D}_k^{-1} d_k$  with  $\tau_k > 0$ , and let

$$\eta_k = \prod_{j=2}^k \lambda_{\min}(\mathbf{D}_j^{-1} \mathbf{D}_{j-1}), \quad \bar{f}_*^k := \frac{1}{\rho_k} \sum_{j=1}^k \rho_{j,k} f(x^*, s_j), \quad h_k = \bar{f}_k + \langle d_k, x^k \rangle - \gamma_k.$$

It follows that

$$\max_{j=1,\dots,k} \bar{f}_*^j \geq f_*^{k+1} := \frac{2 \sum_{j=1}^k \eta_j \tau_j h_j - \|x^1 - x^*\|^2 - \sum_{j=1}^k \eta_j \tau_j^2 \|d_j\|_{\mathbf{D}_j^{-1}}^2}{2 \sum_{j=1}^k \eta_j \tau_j \rho_j}. \quad (37)$$

Furthermore we have the recurrence

$$f_*^{k+1} = \frac{f_*^k \sum_{j=1}^{k-1} \eta_j \tau_j \rho_j + \eta_k \tau_k \left( h_k - \frac{1}{2} \tau_k \|d_k\|_{\mathbf{D}_k^{-1}}^2 \right)}{\sum_{j=1}^k \eta_j \tau_j \rho_j}. \quad (38)$$

In particular when  $\mathbf{D}_k = \mathbf{Id}$  for every  $k$ , then we have that  $\eta_k = 1$  for all  $k$ .

*Proof.* From step (36) and re-arranging we have that

$$\begin{aligned} 2 \left( \max_{j=1,\dots,k} \bar{f}_*^j \right) \left( \sum_{j=1}^k \eta_j \tau_j \rho_j \right) &\geq 2 \left( \sum_{j=1}^k \eta_j \tau_j \rho_j \right) \bar{f}_*^j \\ &\geq 2 \sum_{j=1}^k \eta_j \tau_j h_j - \|x^1 - x^*\|_{\mathbf{D}_1}^2 - \sum_{j=1}^k \eta_j \tau_j^2 \|d_j\|_{\mathbf{D}_j^{-1}}^2. \end{aligned}$$

If we now assume that  $\bar{f}_*^j \approx f(x^*)$  (or upper bounding  $\bar{f}_*^j$  by a constant) then by substituting in  $f(x^*)$ , dividing through by  $(\sum_{j=1}^k \eta_j \tau_j \rho_j)$  gives the estimate

$$\max_{j=1,\dots,k} \bar{f}_*^j \geq f_*^{k+1} := \frac{2 \sum_{j=1}^k \eta_j \tau_j h_j - \|x^1 - x^*\|^2 - \sum_{j=1}^k \eta_j \tau_j^2 \|d_j\|_{\mathbf{D}_j^{-1}}^2}{2 \sum_{j=1}^k \eta_j \tau_j \rho_j}.$$

Finally the recurrence follows since

$$\begin{aligned} f_*^{k+1} &= \frac{2 \sum_{j=1}^k \eta_j \tau_j h_j - \|x^1 - x^*\|_{\mathbf{D}_1}^2 - \sum_{j=1}^k \eta_j \tau_j^2 \|d_j\|_{\mathbf{D}_j^{-1}}^2}{2 \sum_{j=1}^k \eta_j \tau_j \rho_j} \\ &= \frac{\sum_{j=1}^{k-1} \eta_j \tau_j \rho_j}{\sum_{j=1}^k \eta_j \tau_j \rho_j} \frac{2 \sum_{j=1}^{k-1} \eta_j \tau_j h_j - \|x^1 - x^*\|_{\mathbf{D}_1}^2 - \sum_{j=1}^{k-1} \eta_j \tau_j^2 \|d_j\|_{\mathbf{D}_j^{-1}}^2}{2 \sum_{j=1}^{k-1} \eta_j \tau_j \rho_j} \\ &\quad + \frac{2 \eta_k \tau_k h_k - \eta_k \tau_k^2 \|d_k\|_{\mathbf{D}_k^{-1}}^2}{2 \sum_{j=1}^k \eta_j \tau_j \rho_j} \\ &= \frac{f_*^k \sum_{j=1}^{k-1} \eta_j \tau_j \rho_j + \eta_k \tau_k \left( h_k - \frac{1}{2} \tau_k \|d_k\|_{\mathbf{D}_k^{-1}}^2 \right)}{\sum_{j=1}^k \eta_j \tau_j \rho_j}. \end{aligned}$$

□

## E. Proofs for Convergence Analysis

Here we give another motivation for a variant of MoMo through convexity. We discovered this interpretation of MoMo after reading the concurrent work (Wang et al., 2023).

For this alternative derivation of MoMo, first let  $\tau_k \geq 0$  be a free parameter, and consider a general momentum method with a preconditioner given by

$$d_k = \sum_{j=1}^k \rho_{j,k} \nabla f(x^j, s_j), \quad x^{k+1} = x^k - \tau_k \mathbf{D}_k^{-1} d_k. \quad (39)$$

We can now view  $x^{k+1}$  as a function of  $\tau_k$ , that is  $x^{k+1}(\tau_k)$ . Ideally we would like to choose  $\tau_k$  so that  $x^{k+1}$  is as close as possible to the optimum solution  $x^*$ , that is to minimize  $\|x^{k+1}(\tau_k) - x^*\|_{\mathbf{D}_k}^2$  in  $\tau_k$ . This is general not possible because we do not know  $x^*$ . But if we assume that  $f(\cdot, s)$  is a convex function, then we can minimize an upper bound of  $\|x^{k+1}(\tau_k) - x^*\|_{\mathbf{D}_k}^2$  with respect to  $\tau_k$ . As we show next, this gives the adaptive term in the learning rate of MoMo if  $f_*^k = \bar{f}_*^k$ .

**Lemma E.1.** Let  $f(\cdot, s)$  be convex for every  $s$ . Let  $h_k := \bar{f}_k + \langle d_k, x^k \rangle - \gamma_k$  where  $d_k, \bar{f}_k$ , and  $\gamma_k$  are defined in (11). Consider the iterates given by (39) and let  $x^* \in \arg \min_{x \in \mathbb{R}^d} f(x)$ . Then, we have the upper bound

$$\|x^{k+1} - x^*\|_{\mathbf{D}_k}^2 \leq \|x^k - x^*\|_{\mathbf{D}_k}^2 - 2\tau_k(h_k - \rho_k \bar{f}_*^k) + \tau_k^2 \|d_k\|_{\mathbf{D}_k^{-1}}^2. \quad (40)$$

The minimum of the right-hand side of (40), over the set  $\tau_k \in \mathbb{R}_{\geq 0}$ , is attained at

$$\bar{\tau}_k = \frac{(h_k - \rho_k \bar{f}_*^k)_+}{\|d_k\|_{\mathbf{D}_k^{-1}}^2}. \quad (41)$$

*Proof.* Subtracting  $x^*$  from both sides, taking norms and expanding the squares gives

$$\|x^{k+1} - x^*\|_{\mathbf{D}_k}^2 = \|x^k - x^*\|_{\mathbf{D}_k}^2 - 2\tau_k \langle d_k, x^k - x^* \rangle + \tau_k^2 \|d_k\|_{\mathbf{D}_k^{-1}}^2. \quad (42)$$

Denote  $\nabla f_j := \nabla f(x^j, s_j)$ ,  $f_j := f(x^j, s_j)$ . Now using that

$$\begin{aligned} \langle d_k, x^k - x^* \rangle &= \sum_{j=1}^k \rho_{j,k} \langle \nabla f_j, x^k - x^* \rangle \\ &= \sum_{j=1}^k \rho_{j,k} (\langle \nabla f_j, x^k - x^j \rangle + \langle \nabla f_j, x^j - x^* \rangle) \\ &\geq \sum_{j=1}^k \rho_{j,k} (\langle \nabla f_j, x^k - x^j \rangle + f_j - f(x^*, s_j)) \quad (\text{by convexity of } f(\cdot, s_j)) \\ &= \langle d_k, x^k \rangle - \gamma_k + \sum_{j=1}^k \rho_{j,k} (f_j - f(x^*, s_j)) = h_k - \rho_k \bar{f}_*^k. \end{aligned} \quad (43)$$

Using (43) in (42) gives

$$\begin{aligned} \|x^{k+1} - x^*\|_{\mathbf{D}_k}^2 &= \|x^k - x^*\|_{\mathbf{D}_k}^2 - 2\tau_k \langle d_k, x^k - x^* \rangle + \tau_k^2 \|d_k\|_{\mathbf{D}_k^{-1}}^2 \\ &\leq \|x^k - x^*\|_{\mathbf{D}_k}^2 - 2\tau_k (h_k - \rho_k \bar{f}_*^k) + \tau_k^2 \|d_k\|_{\mathbf{D}_k^{-1}}^2. \end{aligned}$$

If we now minimize the right-hand side of the above in  $\tau_k$ , but restricted to  $\tau_k \geq 0$ , we arrive at (41).  $\square$

Inequality (40) holds for any choice of  $\tau_k \geq 0$  in (39), in particular for  $\tau_k = \min\{\frac{\alpha_k}{\rho_k}, \frac{(h_k - \rho_k \bar{f}_*^k)_+}{\|d_k\|_{\mathbf{D}_k^{-1}}^2}\}$ . This choice for  $\tau_k$  is equal to MoMo for  $\lambda = 0$  and  $f_*^k = \bar{f}_*^k$ . As a consequence, we we can prove a descent lemma for MoMo.

**Lemma 5.1.** Let  $f(\cdot, s)$  be convex for every  $s$  and let  $x^* \in \arg \min_{x \in \mathbb{R}^d} f(x)$ . For the iterates of the general MoMo update (cf. Lemma 3.1) with  $\lambda = 0$  and  $f_*^k = \bar{f}_*^k$ , it holds

$$\|x^{k+1} - x^*\|_{\mathbf{D}_k}^2 \leq \|x^k - x^*\|_{\mathbf{D}_k}^2 - \tau_k (h_k - \rho_k \bar{f}_*^k)_+. \quad (20)$$

*Proof.* We again denote  $h_k = \bar{f}_k + \langle d_k, x^k \rangle - \gamma_k$ . First, assume  $\tau_k = \frac{(h_k - \rho_k \bar{f}_*^k)_+}{\|d_k\|_{\mathbf{D}_k^{-1}}^2}$ . Inserting this  $\tau_k$  back in (40) we have that

$$\begin{aligned} \|x^{k+1} - x^*\|_{\mathbf{D}_k}^2 &\leq \|x^k - x^*\|_{\mathbf{D}_k}^2 - 2 \frac{(h_k - \rho_k \bar{f}_*^k)_+}{\|d_k\|_{\mathbf{D}_k^{-1}}^2} (h_k - \rho_k \bar{f}_*^k) + \frac{(h_k - \rho_k \bar{f}_*^k)_+^2}{\|d_k\|_{\mathbf{D}_k^{-1}}^2} \\ &= \|x^k - x^*\|_{\mathbf{D}_k}^2 - \frac{(h_k - \rho_k \bar{f}_*^k)_+^2}{\|d_k\|_{\mathbf{D}_k^{-1}}^2} \\ &= \|x^k - x^*\|_{\mathbf{D}_k}^2 - \tau_k (h_k - \rho_k \bar{f}_*^k)_+. \end{aligned} \quad (44)$$

Here we used that  $a(a)_+ = (a)_+^2$  for all  $a \in \mathbb{R}$ .

If we have  $\tau_k = \frac{\alpha_k}{\rho_k}$ , then from (40) we get

$$\|x^{k+1} - x^*\|_{\mathbf{D}_k}^2 \leq \|x^k - x^*\|_{\mathbf{D}_k}^2 + \frac{\alpha_k}{\rho_k} [-2(h_k - \rho_k \bar{f}_*^k) + \alpha_k \|d_k\|_{\mathbf{D}_k^{-1}}^2]. \quad (45)$$

In this case  $\frac{\alpha_k}{\rho_k} \leq \frac{(h_k - \rho_k \bar{f}_*^k)_+}{\|d_k\|_{\mathbf{D}_k^{-1}}^2}$  and hence  $\frac{\alpha_k}{\rho_k} \|d_k\|_{\mathbf{D}_k^{-1}}^2 \leq (h_k - \rho_k \bar{f}_*^k)_+$ . Further, it must hold  $(h_k - \rho_k \bar{f}_*^k) = (h_k - \rho_k \bar{f}_*^k)_+$  as  $\alpha_k > 0$ . We get

$$\begin{aligned} \|x^{k+1} - x^*\|_{\mathbf{D}_k}^2 &\leq \|x^k - x^*\|_{\mathbf{D}_k}^2 - \frac{\alpha_k}{\rho_k} (h_k - \rho_k \bar{f}_*^k)_+ \\ &= \|x^k - x^*\|_{\mathbf{D}_k}^2 - \tau_k (h_k - \rho_k \bar{f}_*^k)_+ \quad (\tau_k = \frac{\alpha_k}{\rho_k}). \end{aligned} \quad (46)$$

Now, if  $\tau_k = \min\{\frac{\alpha_k}{\rho_k}, \frac{(h_k - \rho_k \bar{f}_*^k)_+}{\|d_k\|_{\mathbf{D}_k^{-1}}^2}\}$ , either (44) or (46) is true, and hence we have

$$\|x^{k+1} - x^*\|_{\mathbf{D}_k}^2 \leq \|x^k - x^*\|_{\mathbf{D}_k}^2 - \tau_k (h_k - \rho_k \bar{f}_*^k)_+.$$

□

Recall the interpolation condition (21), given by

$$f(x^*, s) = \inf_x f(x, s) = f^* \quad \text{for all } s \in \mathcal{D}.$$

**Theorem 5.2.** Let  $f(\cdot, s)$  be convex for every  $s$  and let  $x^* \in \arg \min_{x \in \mathbb{R}^d} f(x)$ . Assume that (21) holds. Let  $(x^k)$  be the iterates of Algorithm 1 with  $f_*^k = f^*$ ,  $\alpha_k = +\infty$  for all  $k \in \mathbb{N}$  and assume that  $d_k \neq 0$  for all  $k \in \mathbb{N}$ . Define

$$B := \{x \mid \|x - x^*\| \leq \|x^1 - x^*\|\}.$$

Assume that there exists  $G > 0$  such that  $\max_{x \in B} \mathbb{E} [\|\nabla f(x, s)\|^2] = G^2 < \infty$ . Then, it holds

$$\min_{k=1, \dots, K} \mathbb{E} [f(x^k) - f^*] \leq \frac{G \|x^1 - x^*\|}{\sqrt{K} (1 - \beta)}.$$

*Proof.* Recall that Algorithm 1 is Lemma 3.1 with  $\rho_k = 1$ ,  $\mathbf{D}_k = \mathbf{I}_d$  and  $\lambda = 0$ . The key quantity is  $h_k = \bar{f}_k + \langle d_k, x^k \rangle - \gamma_k$ . Let us denote  $g_k = \nabla f(x^k, s_k)$ . Further, denote with  $\mathcal{F}_k$  the  $\sigma$ -algebra generated by  $\{s_1, \dots, s_{k-1}\}$ .

**Step 1.** We first show by induction that  $h_k - f^* \geq 0$  for all  $k \in \mathbb{N}$ . For  $k = 1$  we have  $h_1 = f(x^1, s_1) \geq f^*$  due to (21). Now, for  $k \geq 2$ , assume that  $h_{k-1} - f^* \geq 0$ . Rewrite as

$$\begin{aligned} h_k &= \beta [\bar{f}_{k-1} + \langle d_{k-1}, x^k \rangle - \gamma_{k-1}] + (1 - \beta) [f(x^k, s_k) + \langle g_k, x^k \rangle - \langle g_k, x^k \rangle] \\ &= \beta [\bar{f}_{k-1} + \langle d_{k-1}, x^{k-1} \rangle - \gamma_{k-1} + \langle d_{k-1}, x^k - x^{k-1} \rangle] + (1 - \beta) f(x^k, s_k) \\ &= \beta h_{k-1} + \beta \langle d_{k-1}, x^k - x^{k-1} \rangle + (1 - \beta) f(x^k, s_k). \end{aligned}$$

Using the update rule  $x^k = x^{k-1} - \tau_{k-1}d_{k-1}$  in the above gives

$$h_k = \beta(h_{k-1} - \tau_{k-1}\|d_{k-1}\|^2) + (1 - \beta)f(x^k, s_k). \quad (47)$$

Recall that  $\tau_k = \frac{(h_k - f^*)_+}{\|d_k\|^2}$  due to  $\alpha_k = +\infty$ . Hence,

$$\tau_{k-1}\|d_{k-1}\|^2 = (h_{k-1} - f^*_{k-1})_+ = (h_{k-1} - f^*)_+ = h_{k-1} - f^*$$

where the last equality is the induction hypothesis. Re-arranging the above we get

$$h_{k-1} - \tau_{k-1}\|d_{k-1}\|^2 = f^*. \quad (48)$$

Plugging this equality into (47) gives

$$h_k = \beta f^* + (1 - \beta)f(x^k, s_k) \geq f^*,$$

due to  $\beta \in [0, 1)$  and  $f(x^k, s_k) \geq f^*$ . This completes the induction, and we have further shown that

$$h_k - f^* = (1 - \beta)(f(x^k, s_k) - f^*). \quad (49)$$

**Step 2.** Due to (21) and  $\rho_k = 1$ , it holds  $\bar{f}_k^* = f^* = f_k^*$ . Hence, the assumptions of Lemma 5.1 are satisfied and we can apply (20), which implies in particular that the iterates  $(x^k)$  are almost surely contained in the bounded set  $B$ . By assumption, we conclude that  $\mathbb{E}[\|g_j\|^2 | \mathcal{F}_k] \leq G^2$  for all  $j \leq k$ . Using Jensen for the discrete probability measure induced by  $\rho_{j,k}$ , we have

$$\|d_k\|^2 = \left\| \sum_{j=1}^k \rho_{j,k} g_j \right\|^2 \leq \sum_{j=1}^k \rho_{j,k} \|g_j\|^2.$$

Thus, we conclude for the conditional expectation that  $\mathbb{E}[\|d_k\|^2 | \mathcal{F}_k] \leq G^2$ . By Step 1, we have  $\tau_k = \frac{h_k - f^*}{\|d_k\|^2}$ . We will use next that  $(x, y) \mapsto x^2/y$  is convex for  $x \in \mathbb{R}, y > 0$ . From (44) and applying conditional expectation, we have

$$\begin{aligned} \mathbb{E}[\|x^{k+1} - x^*\|^2 | \mathcal{F}_k] &\leq \|x^k - x^*\|^2 - \mathbb{E}\left[\frac{(h_k - f^*)^2}{\|d_k\|^2} | \mathcal{F}_k\right] \\ &\leq \|x^k - x^*\|^2 - \frac{\mathbb{E}[h_k - f^* | \mathcal{F}_k]^2}{\mathbb{E}[\|d_k\|^2 | \mathcal{F}_k]} \\ &\stackrel{(49)}{=} \|x^k - x^*\|^2 - \frac{(1 - \beta)^2 \mathbb{E}[f(x^k, s_k) - f^* | \mathcal{F}_k]^2}{\mathbb{E}[\|d_k\|^2 | \mathcal{F}_k]} \\ &\leq \|x^k - x^*\|^2 - \frac{(1 - \beta)^2 (f(x^k) - f^*)^2}{G^2}. \end{aligned}$$

**Step 3.** Taking full expectation, using the law of total expectation, summing over  $k = 1, \dots, K$ , dividing by  $K$  and re-arranging gives

$$\frac{1}{K} \sum_{k=1}^K \mathbb{E}[(f(x^k) - f^*)^2] \leq \frac{G^2 \|x^1 - x^*\|^2}{K(1 - \beta)^2}. \quad (50)$$

Now, due to Jensen's inequality we have  $\mathbb{E}[(f(x^k) - f^*)^2] \geq \mathbb{E}[f(x^k) - f^*]^2$  and because the square-root is concave, it holds

$$\frac{1}{K} \sum_{k=1}^K \mathbb{E}[f(x^k) - f^*] \leq \sqrt{\frac{1}{K} \sum_{k=1}^K \mathbb{E}[f(x^k) - f^*]^2}.$$

Using the above together with (50), we obtain

$$\min_{k=1, \dots, K} \mathbb{E}[f(x^k) - f^*] \leq \frac{1}{K} \sum_{k=1}^K \mathbb{E}[f(x^k) - f^*] \leq \frac{G \|x^1 - x^*\|}{\sqrt{K}(1 - \beta)}.$$

□

The above result is basically identical to (Loizou et al., 2021, Thm. C.1), but also allowing for momentum. We make two remarks: the best constant is clearly achieved by  $\beta = 0$ , i.e. no momentum. While empirically, momentum helps in most cases, we can not show a theoretical improvement at this time. Second, we do not need to assume bounded gradient norms as done in (Loizou et al., 2021), because this follows from the descent property Lemma 5.1. However, this improvement could be achieved analogously for the the proof of (Loizou et al., 2021) based on the techniques we developed here.

## F. Additional Information on Experiments

### F.1. Additional Plots

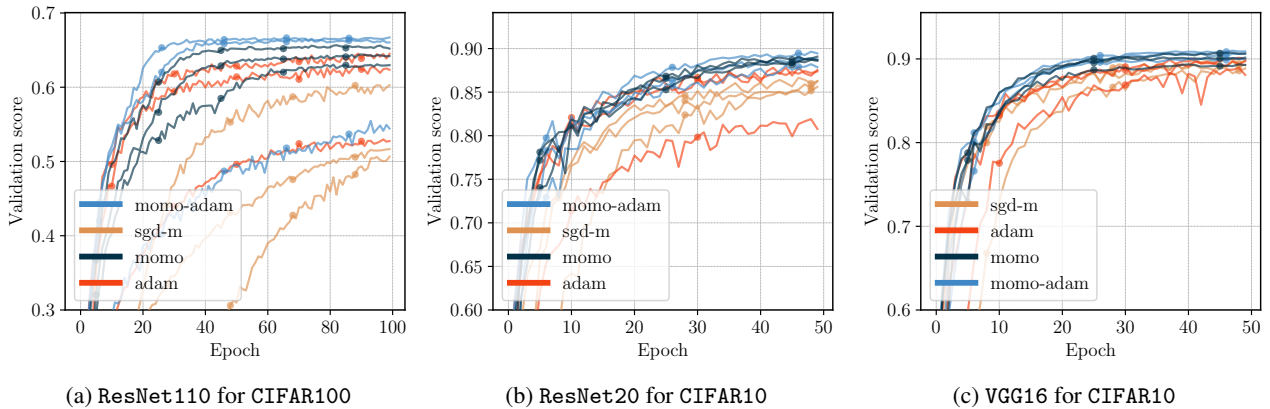


Figure F.1. Validation score over training, we plot, for each method, the three choices of  $\alpha_0$  that lead to the best validation score (compare to Figures 2 and F.3).

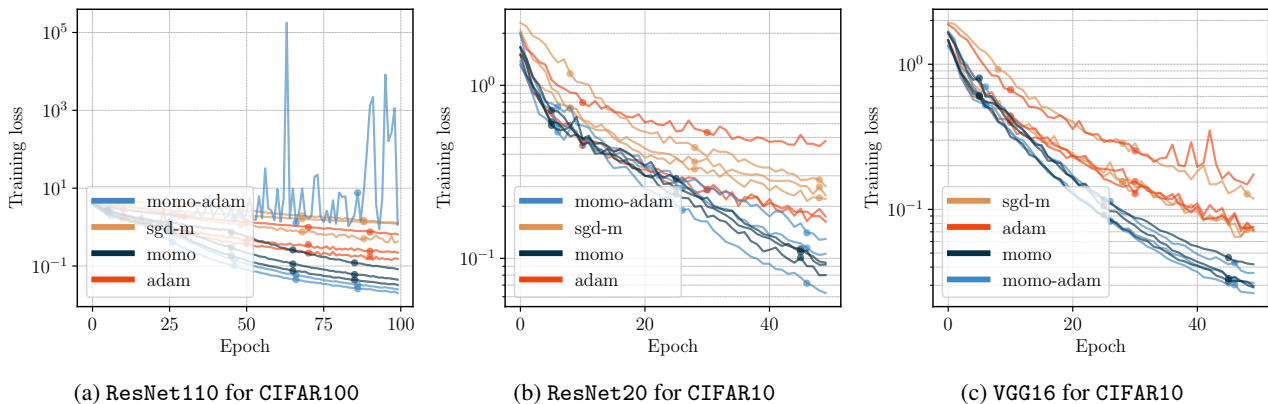


Figure F.2. Training loss over training, we plot, for each method, the three choices of  $\alpha_0$  that lead to the best validation score.

### F.2. Experimental Setup of Section 6.1

We set the momentum parameter  $\beta = 0.9$  for MoMo and SGD-M, and  $(\beta_1, \beta_2) = (0.9, 0.999)$  for MoMo-Adam and Adam respectively. We do not use weight decay, i.e.  $\lambda = 0$ .

For SGD-M we set the dampening parameter (in Pytorch) equal to the momentum parameter 0.9. Like this, SGD-M does an exponentially-weighted average of past gradients and hence is comparable to MoMo for identical learning rate and momentum. Setting dampening = 0.9 is equivalent to running with dampening = 0 and a ten times smaller learning rate. For all other hyperparameters we use the Pytorch default values for Adam and SGD-M (unless explicitly stated otherwise).



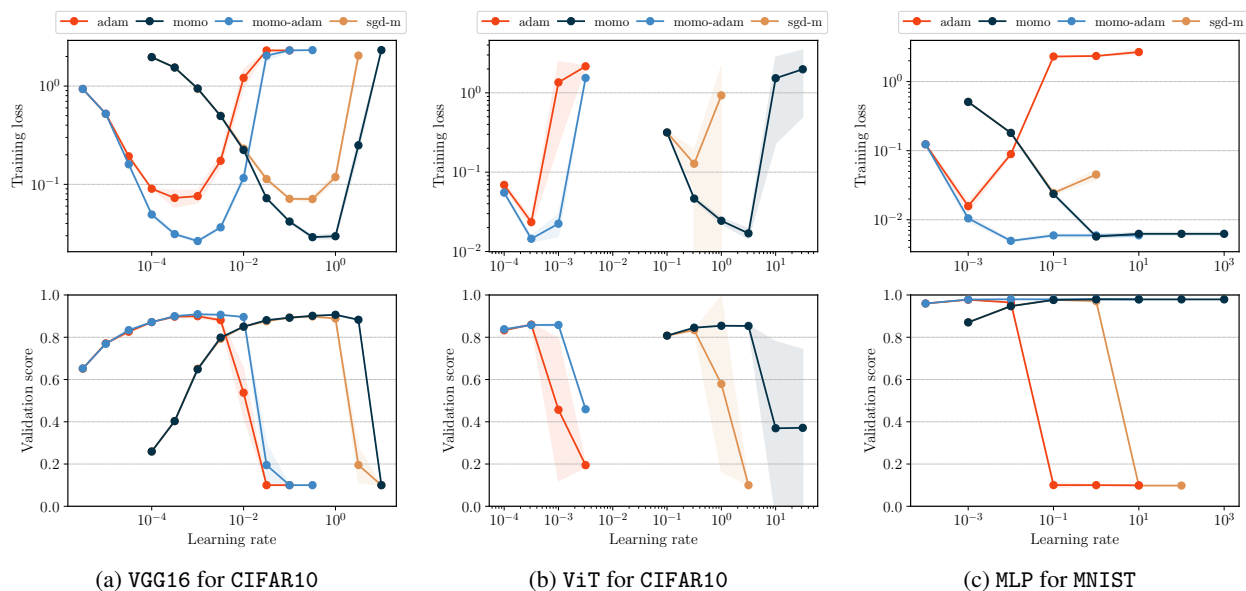


Figure F.3. Training loss (top row) and validation accuracy (bottom row) after a fixed number of epochs, for varying (constant) learning rate  $\alpha_0$ .

### F.3. Models and Datasets

#### ResNet for CIFAR

(He et al., 2016)

Used for ResNet20 for CIFAR10 and ResNet110 for CIFAR100. We adapt the last layer output size to  $\{10, 100\}$  according to the used dataset. We run 50 epochs for ResNet20 and 100 epochs for ResNet110, both with batch size 128.

Model [https://github.com/akamaster/pytorch\\_resnet\\_cifar10/blob/master/resnet.py](https://github.com/akamaster/pytorch_resnet_cifar10/blob/master/resnet.py)

#### VGG16 for CIFAR10

(Simonyan & Zisserman, 2015)

A deep network with 16 convolutional layers. We run 50 epochs with batch size 128.

Model <https://github.com/chengyangfu/pytorch-vgg-cifar10/blob/master/vgg.py>

#### ViT for CIFAR10

(Dosovitskiy et al., 2021)

A small vision transformer, based on the hyperparameter setting proposed in [github.com/kentaroy47/vision-transformers-cifar10](https://github.com/kentaroy47/vision-transformers-cifar10). In particular, we set the patch size to four. We run 200 epochs with batch size 512.

Model <https://github.com/lucidrains/vit-pytorch>

#### ResNet18 for Imagenet32

(He et al., 2016)

Imagenet32 is a downsampled version of Imagenet-1k to images of  $32 \times 32$  pixels. We adapt the last layer output size to 1000. We run 45 epochs with batch size 128.

Model <https://github.com/kuangliu/pytorch-cifar/blob/master/models/resnet.py>

#### ResNet18 for Imagenet-1k

(He et al., 2016)

We use both a constant learning rate and a schedule that decays the learning rate by 0.1 every 30 epochs. We run 90 epochs. Note that for SGD-M the decaying schedule with initial learning rate of 0.1 is considered state-of-the-art. As we set dampening = 0.9, and this is equivalent to dampening = 0 and a ten times smaller learning rate (see Appendix F.2), in our plots the best score is displayed for initial learning rate of 1 accordingly.

Model [pytorch.org/vision/main/models/generated/torchvision.models.resnet18.html](https://pytorch.org/vision/main/models/generated/torchvision.models.resnet18.html)

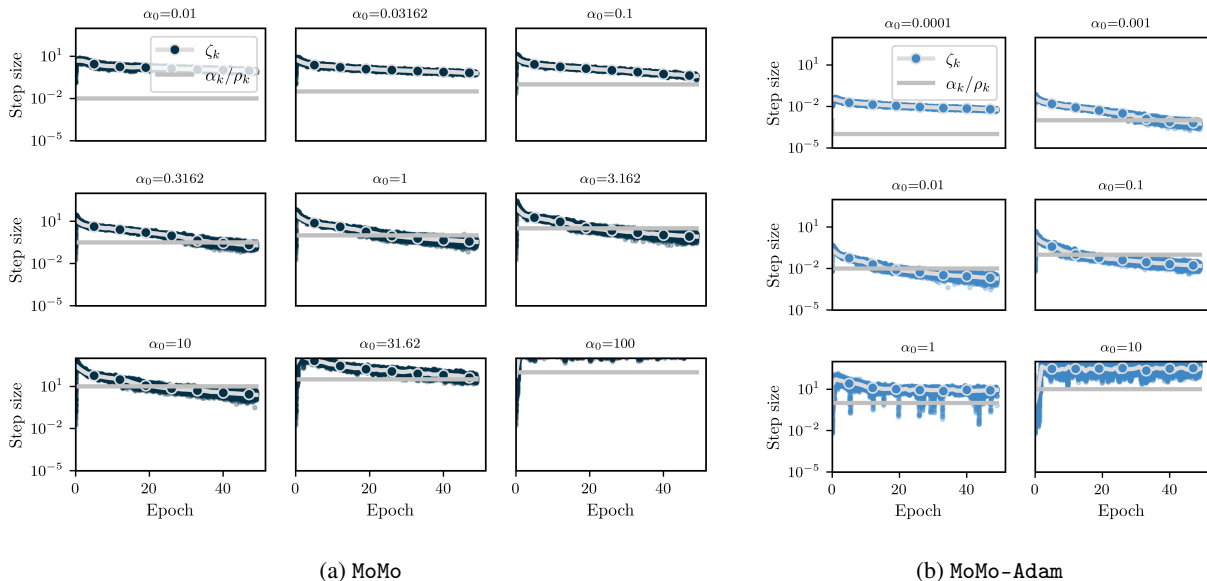


Figure F.4. ResNet20 for CIFAR10. Adaptive learning rate of MoMo (left) and MoMo-Adam (right). The colored dots represent the term  $\zeta_k$  in each iteration. The grey line represents the user-specified learning rate  $\alpha_k/\rho_k$  (note that  $\rho_k = 1$  for MoMo and  $\rho_k \approx 1$  except for the first few iterations in MoMo-Adam). The minimum of the grey line and the dots is the adaptive learning rate  $\tau_k = \min\{\frac{\alpha_k}{\rho_k}, \zeta_k\}$  in each iteration. The silver line with colored markers is the median over the values of  $\zeta_k$  in each epoch.

**DLRM for Criteo**

(Tien & Chapelle, 2014)

DLRM is an industry-scale model with over 300 million parameters. the Criteo dataset contains approximately 46 million training samples. We run 300k iterations with batch size 128.

Dataset <https://kaggle.com/c/criteo-display-ad-challenge>

Model <https://github.com/facebookresearch/dlrm>

**IWSLT14**

(Ott et al., 2019)

We use a transformer with six encoder and decoder blocks from fairseq. The training loss is the cross-entropy loss with label smoothing of 0.1. We use weight decay of  $\lambda = 10^{-4}$  (although we noticed that weight decay does not influence the performance of MoMo-Adam), momentum parameters  $(\beta_1, \beta_2) = (0.9, 0.98)$ . We train for 60 epochs.

Model <https://github.com/facebookresearch/fairseq>

**UNet for Smithsonian Butterflies**

(Ronneberger et al., 2015)

The Smithsonian Butterflies dataset contains 1,000 images of butterflies. We train a diffusion model, using a UNet2D architecture from the Huggingface library. For both constant learning-rate schedule as well as cosine decay we use a warmup period, where the learning rate is increased linearly over 500 steps from zero to the final value. For MoMo-Adam we use no weight decay. For Adam we tried both  $\lambda \in \{0, 0.01\}$  but did not observe major differences; we display the results for  $\lambda = 0.01$  (the default value). We train for 50 epochs with batch size 16. The training script is adapted from [https://colab.research.google.com/github/huggingface/notebooks/blob/main/diffusers\\_doc/en/pytorch/basic\\_training.ipynb](https://colab.research.google.com/github/huggingface/notebooks/blob/main/diffusers_doc/en/pytorch/basic_training.ipynb).

Dataset [https://huggingface.co/datasets/huggan/smithsonian\\_butterflies\\_subset](https://huggingface.co/datasets/huggan/smithsonian_butterflies_subset)

Model <https://huggingface.co/docs/diffusers/main/en/api/models/unet2d>

**ViT for Imagenet-1k**

(Dosovitskiy et al., 2021)

We train a vision transformer for image classification on the full Imagenet-1k dataset. We use the timm library for training and select the vit\_tiny\_patch16\_224 model. We use the settings reported in (Defazio & Mishchenko, 2023a);

Table 1. Validation score (with one standard deviation) for the best learning rate choice for each method among the ones displayed in Section 6. Symbol “\*” indicates usage of online lower bound, otherwise MoMo(-Adam) used with  $f_*^k = 0$ . Bold indicates the best method (for experiments with multiple seeds, we only mark in bold if the advantage is outside of standard deviation).

	MoMo	MoMo-Adam	SGD-M	Adam(W)
ResNet110 for CIFAR100	65.21 $\pm$ 1.61	<b>66.71</b> $\pm$ 0.31	60.28 $\pm$ 0.36	64.5 $\pm$ 1.14
ResNet20 for CIFAR10	89.07 $\pm$ 0.2	<b>89.45</b> $\pm$ 0.17	86.27 $\pm$ 0.67	87.54 $\pm$ 0.26
ViT for CIFAR10	85.43 $\pm$ 0.19	85.81 $\pm$ 0.57	83.39 $\pm$ 0.28	86.02 $\pm$ 0.44
VGG16 for CIFAR10	90.64 $\pm$ 0.18	<b>90.9</b> $\pm$ 0.17	89.81 $\pm$ 0.43	89.95 $\pm$ 0.67
MLP for MNIST	<b>97.97</b> $\pm$ 0.08	97.96 $\pm$ 0.12	97.73 $\pm$ 0.12	97.75 $\pm$ 0.06
DLRM for Criteo	78.83 $\pm$ 0.038	78.98 $\pm$ 0.036	78.81 $\pm$ 0.041	<b>79.05</b> $\pm$ 0.014
ResNet18 for Imagenet32	<b>47.66</b> *	47.54*	47.38	46.98
ResNet18 for Imagenet-1k	<b>69.68</b>	N/A	69.57	N/A
IWSLT14 (dp 0.1)	N/A	<b>33.63</b> *	N/A	32.56
IWSLT14 (dp 0.3)	N/A	<b>35.34</b> *	N/A	34.97
ViT for Imagenet-1k	N/A	<b>73.83</b> $\pm$ 0.36	N/A	72.83 $\pm$ 0.51

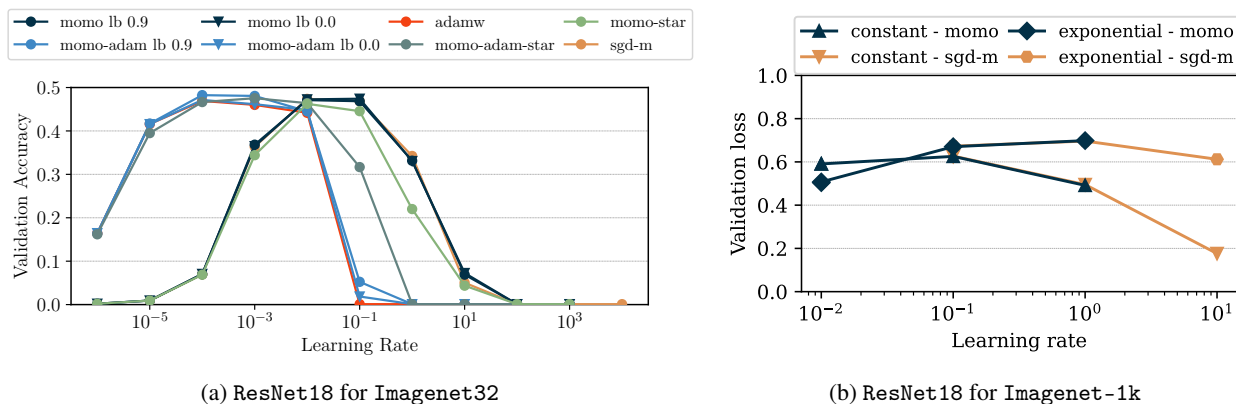


Figure F.5. Left: Validation accuracy of a ResNet18 for Imagenet32 with weight decay  $\lambda = 10^{-4}$ . Right: Validation accuracy of a ResNet18 for Imagenet-1k, with standard exponential learning rate schedule (decay factor 10 at epochs 30 and 60) and constant learning rate schedule.

the only exception is that when increasing the learning rate  $\alpha$ , we decrease the weight decay  $\lambda$  by the same factor, such that  $\alpha \cdot \lambda = 10^{-4}$  for all runs. By standard practice, we use a warmup period of five epochs (starting at  $10^{-5}$  with epoch-wise steps) to a base learning rate  $\alpha_{\text{base}}$ , followed by a cosine decay. We train for 200 epochs with batch size 512. The loss function is the binary cross entropy loss with label smoothing of 0.1 (also used in (Defazio & Mishchenko, 2023a)).

Model `timm/models/vision_transformer.py`

For each experiments, we list how long one training run approximately takes on the hardware we use. Unless specified otherwise, we train on a single NVIDIA A100 GPU. ResNet110 for CIFAR100 90 min, ResNet20 for CIFAR10 30 min, VGG16 for CIFAR10 30 min, MLP for MNIST 3 min, ViT for Imagenet-1k 10 h (on four NVIDIA A100), UNet for Smithsonian Butterflies 30 min, ResNet18 for Imagenet32 20 hours (on NVIDIA V100), Transformer for IWSLT14 3 hours.

#### F.4. Additional Experiments

We present additional comparisons in Figure F.6, including AdaBelief (Zhuang et al., 2020), AdaBound (Luo et al., 2019), and Lion (Chen et al., 2023). For ResNet110 on CIFAR100, we also tried SGD-M with a learning-rate schedule that decays

by a factor of 0.7 every 30 epochs. This apparently does not yield improvements.

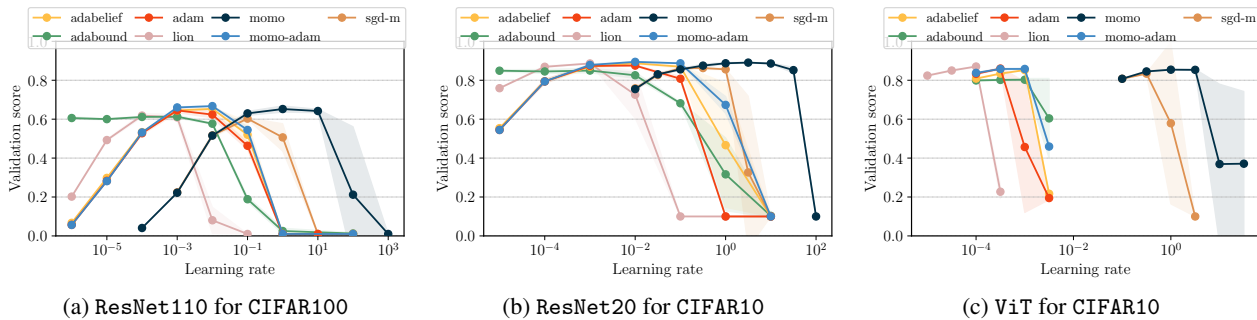


Figure F.6. Additional comparisons to AdaBelief and AdaBound. For CIFAR100 (left plot), the dashed line of SGD-M displays result of using a learning-rate schedule that decays by a factor of 0.7 every 30 epochs.

We present the results for the UNet for Smithsonian Butterflies experiment in Figures F.7 and F.8. We try a constant learning rate, as well as a cosine-decay schedule (both schedules with warmup). The cosine decay works better in general.

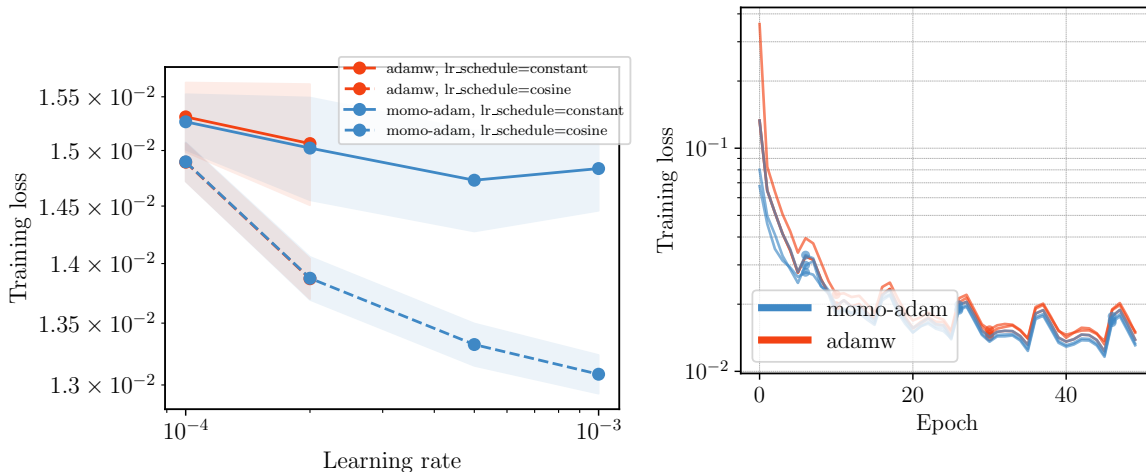


Figure F.7. UNet for Smithsonian Butterflies Left: Stability over learning rate, for constant and cosine decay schedule (more details on schedule settings in Appendix F.3). Values are averaged over three repetitions with different seeds, shaded area depicts one standard deviation. Missing points for Adam mean that at least one of the three repetitions results in NaN loss. Right: Training loss curve for the best three settings (across all base learning rates and both schedules) for each method.

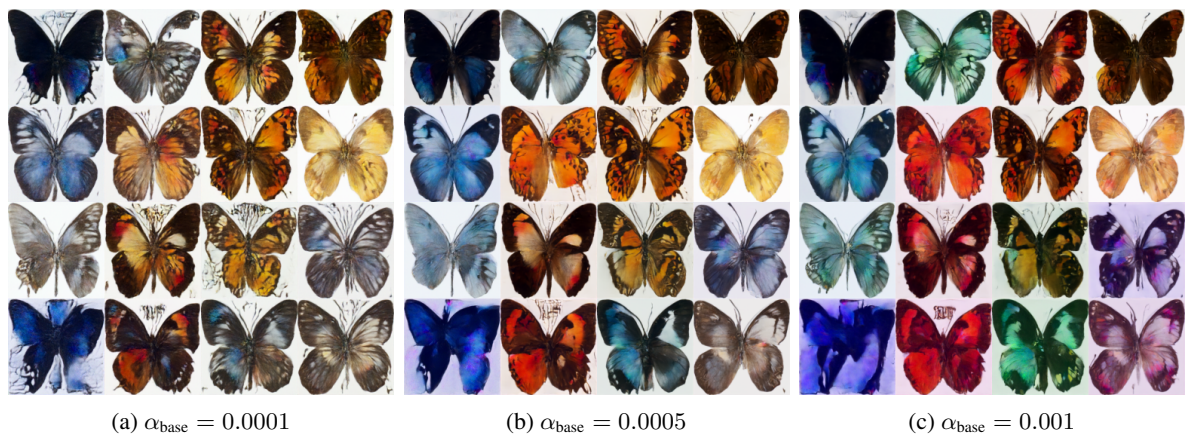


Figure F.8. UNet for Smithsonian Butterflies: Generated images of the UNet diffusion model at the end of training with MoMo-Adam. We display three different base learning rates for the cosine decay schedule (i.e. the displayed value of  $\alpha_{\text{base}}$  corresponds to the  $x$ -axis in the left plot of Figure F.7). Note that when training with Adam, the images in (a) look very similar, but for (b) and (c), Adam diverges and thus the model generates no useful images.

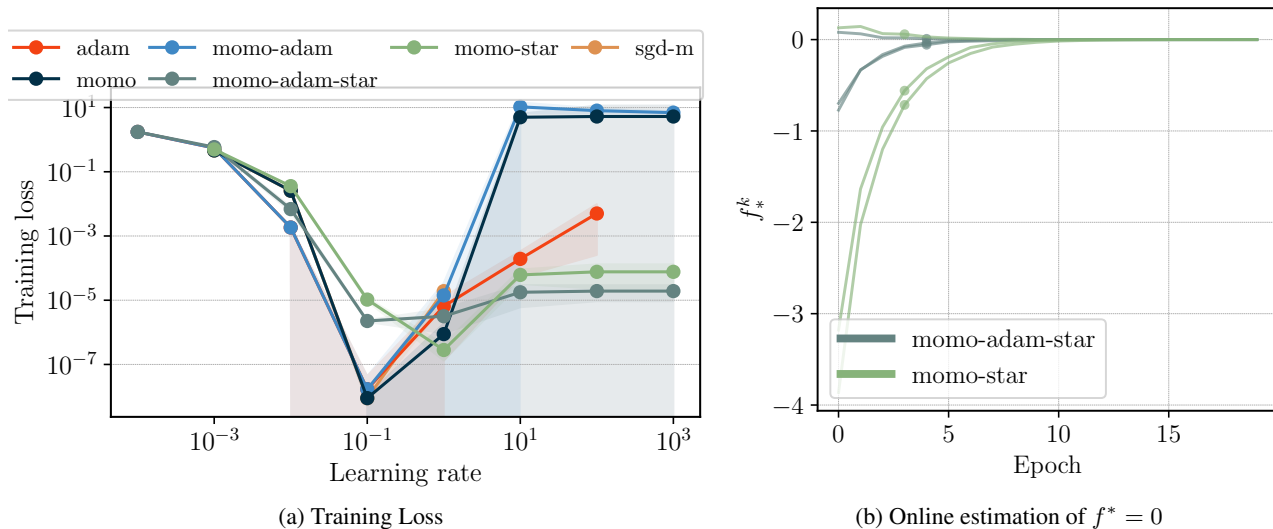


Figure F.9. Illustrative example of online lower bound estimation. For all MoMo methods, we initialize  $f_*^1 = -10$ . Left: Training loss for varying (constant) learning rate  $\alpha_0$ . Right: Value of  $f_*^k$  over training, one line corresponds to one choice of  $\alpha_0$ . We plot per method the four values of  $\alpha_0$  that lead to smallest training loss.

### F.5. Illustrative Example of Online Lower Bound Estimation

We show how our online estimation of  $f_*^k$ , derived in Section 4 and Lemma 4.1, work for a simple example. Consider a regression problem, with synthetic matrix  $A \in \mathbb{R}^{200 \times 10}$  and  $b \in \mathbb{R}^{200}$ . We solve the problem  $\min_{x \in \mathbb{R}^{10}} \sum_{i=1}^{200} \frac{1}{2} \|a_i^\top x - b_i\|^2$ , where  $a_i$  are the rows of  $A$ . The data is generated in a way such that there exists  $\hat{x}$  with  $b = A\hat{x}$  and hence the optimal value is  $f_* = 0$ .

We now run MoMo(-Adam) with lower bound estimate  $f_*^k = -10$  in all iterations, and MoMo(-Adam)\* with initialization  $f_*^1 = -10$ . Clearly, this is not a tight estimate of the optimal value  $f_*$ . From Figure F.9a, we see that online estimation of  $f_*^k$ , used in MoMo(-Adam)\*, improves stability of the training compared to plain MoMo(-Adam) where a constant value  $f_*^k = -10$  is used. From Figure F.9b, we also see that the online values of  $f_*^k$  converge to  $f_* = 0$ .